IMPROVED PORPERTIES OF POLY(LACTIC ACID) WITH INCORPORATION OF CARBON HYBRID NANOSTRUCTURE

Junseok Kim

Thesis submitted to the faculty of the Virginia Polytechnic Institute and State University
in partial fulfillment of the requirements for the degree of

Master of Science
In
Forest Products

Young Teck Kim
Scott H. Renneckar
Seul Yi Lee

26 February 2016
Blacksburg, VA

Keywords: poly(lactic acid), graphene oxide, single-walled carbon nanotube, carbon hybrid nanostructure, coagulation, dispersion, thermal behavior, morphology, light transmittance, mechanical strength, crystalline, oxygen barrier property,

IMPROVED PORPERTIES OF POLY(LACTIC ACID) WITH INCORPORATION OF CARBON HYBRID NANOSTRUCTURE

Junseok Kim

ABSTRACT

Poly(lactic acid) is biodegradable polymer derived from renewable resources and non-toxic, which has become most interested polymer to substitute petroleum-based polymer. However, it has low glass transition temperature and poor gas barrier properties to restrict the application on hot contents packaging and long-term food packaging. The objectives of this research are: (a) to reduce coagulation of graphene oxide/single-walled carbon nanotube (GOCNT) nanocomposite in poly(lactic acid) matrix and (b) to improve mechanical strength and oxygen barrier property, which extend the application of poly(lactic acid).

Graphene oxide has been found to have relatively even dispersion in poly(lactic acid) matrix while its own coagulation has become significant draw back for properties of nanocomposite such as gas barrier, mechanical properties and thermo stability as well as crystallinity. Here, single-walled carbon nanotube was hybrid with graphene oxide to reduce irreversible coagulation by preventing van der Waals of graphene oxide. Mass ratio of graphene oxide and carbon nanotube was determined as 3:1 at presenting greatest performance of preventing coagulation. Four different weight percentage of GOCNT nanocomposite, which are 0.05, 0.2, 0.3 and 0.4 weight percent, were composited with poly(lactic acid) by solution blending method. FESEM morphology determined minor coagulation of GOCNT nanocomopsite for different weight percentage composites. Insignificant crystallinity change was observed in DSC and XRD data. At 0.4 weight percent, it prevented most of UV-B light but was least transparent. GOCNT nanocomposite weight percent was linearly related to ultimate tensile strength of nanocomposite film. The greatest ultimate tensile strength was found at 0.4 weight percent which is 175% stronger than neat poly(lactic acid) film. Oxygen barrier property was improved as GOCNT weight percent increased. 66.57% of oxygen transmission rate was reduced at 0.4 weight percent compared to neat poly(lactic acid). The enhanced oxygen barrier property was ascribed to the outstanding impermeability of hybrid structure GOCNT as well as the strong interfacial adhesion of GOCNT and poly(lactic acid) rather than change of crystallinity. Such a small amount of GOCNT nanocomposite improved mechanical strength and oxygen barrier property while there were no significant change of crystallinity and thermal behavior found.

AKNOWLEDGEMENTS

I would like to thank my advisor Dr. Young Teck Kim, for his advice, suggestion, time, and patience. It has been honor to work within his research group for last two years. Thanks to Dr. Scott H. Renneckar for serving on my committee member as well as understanding of my research and suggestions.

Special thanks to Dr. Seul Yi Lee for educating and broadening my knowledge into graphene world. Also thanks to Dr. Katia Rodriguez for her advice. Special thanks to my graduate fellow Elham Mohammad and Naerin Baek as bring with idea on the research.

A warm thanks to my family especially my wife Melanie Y. Kwon who always supported me. I cannot ask any more than what they have given to me for my entire life. As a dentist, my father Song Ok Kim always motivated and inspired me for my education and career. I appreciated to Dr. Ann Norris for her assistances and instructions on DSC, XRD and TGA. For the last I would like to recognize the Department of Sustainable Biomaterials for financial support for my research.

TABLE OF CONTENTS

LIST OF TABLES AND FIGURES

CHAPTER 1: INTRODUCTION

CHAPTER 2: REVIEW OF LITERATURE

CHAPTER 3: IMPROVED PROPOERTIES OF POLY(LACTIC ACID) WITH INCORPORATION OF CARBON HYBRID NANOSTRUCTURE

LIST OF ABBREVIATIONS AND TERMS

$\%\chi_c$	Percent Crystallinity
ASTM	American Society for Testing and Materials
CNT	Carbon Nanotube
CVD	Chemical Vapor Deposition
DSC	Differential Scanning Calorimetry
E	Young's Modulus
EDS	Energy Dispersive X-ray Spectrometry
FESEM	Field Emission Sacnning Electron Microscope
GO	Graphene Oxide
GOCNT	Graphene Oxide/Carbon Nanotube
K_g	Nuclei of Critical Size
LCA	Life Cycle Assessment
MPa	Megapascal
MWCNT	Multiwall Carbon Nanotube
OTR	Oxygen Transmission Rate
PLA	Poly(lactic acid)
PLA-GOCNT	Poly(lactic acid)/GOCNT
PLGA	Poly(D,L-lactic-co-glycolic acid)
PLLA	Poly(L-lactic acid)
rGO	Reduced Graphene Oxide
SCFs	Supercritical Fluids
SWCNT	Single-walled Carbon Nanotube
T_c	Crystallization Temperature
T_g	Glass Transition Temperature
T_m	Melting Temperature
UTS	Ultimate Tensile Strength
XRD	X-ray Diffraction
ΔH_c	Enthalpy Change at Crystallization Temperature
ΔH_m	Enthlpy of Fusion at Melting Temperature
ΔH_{mc}	Enthalpy of 100% crystalline
σ_e	Folding Surface Free Energy

CHAPTER 1: INTRODUCTION

State of Biodegradable Polymer Industry

Biodegradable polymer industry has increased consumption worth over 3,668.6 Million USD recently. Due to uncertainty of petroleum resources, biodegradable polymer industry has been drastically getting interest. North America which has the largest market in the world consumed around one third of demands. Increasing concern on sustainability of environment and concern on human health break out potential growth of biodegradable polymer industry especially in packaging, automotive and medical area (Norazlina and Kamal 2015).

Biodegradable polymers have renewable, biodegradable, sustainable, and recyclable aspects that possibly substitute petroleum based products in packaging industry and medical industry. Besides these advantages, biodegradable polymers are derived from wood wastes, residues, grasses, crops by-products and crops wastes which reduce the solid waste disposal issues (Mohanty, Misra et al. 2000). Plastics and fibers derived from crops and plants has become novel materials in these days. Now the growth moving of bioplastics and plant derived fibers increases the sales growth around 20 to 30% per year and becomes strongest competence of regular plastics (Scott 2000).

One of the greatest challenges on application in real life is uncertainty on performance as structural and functional. Biodegradable polymers should remain stable on performance during storage and usage. Also they have to be degraded after dispose as their intended lifetime (Mohanty, Misra et al. 2002). To do so, biodegradable polymers have to be designed properly depending on application while they have great performance on bio-degradation. The study of designing biodegradable polymer has been widely conducted. Since large consumptions are needed to lead price reduction in market, it is extremely hard for scientists to find the proper application to support their research (Mohanty, Misra et al. 2000).

Comparison of Biodegradable Polymers to Petroleum Based Plastics

Petroleum based plastics have following advantages: (i) cost efficient and high-speed production including well structured infrastructure; (ii) great mechanical properties; (iii) great barrier properties. However, there are number of disadvantages including: (i) depletion of petroleum resources; (ii) increasing the price of petroleum; (iii) toxicity risks of consumer; (iv) environmental concern (Jamshidian, Tehrany et al. 2010). Biodegradable polymers have been motivated from environmental impact. Petroleum based plastics have produced excessive amount of carbon dioxide and caused issue of disposal waste (Gironi and Piemonte 2011). Compared to petroleum based plastics, biodegradable polymers are derived from agriculture raw materials such as starch, wood and cellulose. Total net balance of carbon dioxide can be decreased since carbon dioxide consumption by plant growing can neutralize the carbon dioxide release from waste disposal of biodegradable polymers (Yates and Barlow 2013). In the 2000s, majority of plastics are disposed in landfill. Biodegradable polymers have higher degradation rate due to faster kinetics compared to plastics. Therefore, biodegradable polymers have benefit on reducing volume of landfill. Based on the Life Cycle Assessment (LCA), biodegradable polymers and petroleum based plastics can be compared in following factors: abiotic depletion, global warming, human toxicity, fresh water aquatic ecotoxicity, marine aquatic ecotoxicology, eutrophication, acidification, terrestrial ecotoxcity, and photochemical oxidation (Gironi and Piemonte 2011). Table 1 shows the impact of various type of plastics on global warming (Patel 2002). This table indicates that biodegradable polymers are advantageous on energy demand and emissions of carbon dioxide over petroleum based plastics.

Even though the environmental advantage of biodegradable polymers, there are many obstacles to be solved. Biodegradable polymers are always questioned on availability, processability, cost efficiency, and performance. The physical weakness such as low impact modification, low heat resistance, poor barrier performance and secondary issues including antioxidant, antifog properties have prevented biodegradable polymers to be substitute of petroleum based plastics. Many researchers, recently, have suggested and studied on additives of nanoparticles and polymer blends to improve physical properties of biodegradable polymers. Even if lack of infrastructure of process and disadvantage on physical

properties, researchers have increased interest on renewability and sustainability of biodegradable polymers.

Trend of Biodegradable Polymers Composites and Nanocomposites

While biodegradable polymers are renewable, sustainable and compatible to environment, they present numerous disadvantages as explained above. To improve such disadvantages, researchers studied on various approaches to modify polymers. Usually, polymers are modified in two different way: chemical modification and physical modification. For chemical modification, polymeric back bone has to be modified in either varying functional group of polymer or copolymerizing with other polymers. Furthermore, copolymerization can be done by graft, block, and random copolymers to design specific polymer properties. On the other hand, physical modification can be performed without changing polymeric back-bone but simply by blending and compositing (Dash and Konkimalla 2012).

Recently, researchers have studied on numerous nanoparticles to modify biodegradable polymer. TiO_2 nanoparticles, as a photocatalysist, has been modified to be uniformly distributed on poly(lactic acid) matrix. This research studied on the influence of TiO_2 on poly(lactic acid) and its transparency. Researchers concluded that poly(lactic acid)-TiO_2 nanocompsite's photodegradation has been improved (Nakayama and Hayashi 2007). Bacterial nanofibrils are introduced to poly(lactic acid) and improved transparency of the nanocomposites due to size effect of the nanofibrillar bacterial cellulose. This study also found that tensile strength and Young's modulus of the nanocomposite increased by 203% and 146% respectively (Kim, Jung et al. 2009). Using carbon nanotube as a reinforcing nanofiller has been popular in polymer nanocomposite research. Functionalized carbon nanotube has been composited with poly(lactic acid) and accelerated the crystallization of poly(lactic acid) drastically due to formation of homogeneous and small spherulites (Li, Wang et al. 2009). Modification of polymers with graphene-based nanomaterial has been drastically interested due to its outstanding physical, electrical and thermal properties. However, research has not successfully modified graphene-based nanomaterial into polymers due to significant coagulation itself (Wang, Sun et al. 2011). On the other hand, hybrid nanostructure of graphene-based nanomaterial has been suggested to polymer modification to enhance the dispersion of

graphitic nanomaterial (Lv, Cruz-Silva et al. 2014). To do so, researchers can attempt to predesign desirable biodegradable polymers and achieve improvement on targeted properties.

Research Objectives

The objectives of this research are: (a) to reduce coagulation of graphene oxide/single-walled carbon nanotube (GOCNT) nanocomposite in poly(lactic acid) matrix and (b) to improve mechanical strength and oxygen barrier property, which extend the application of poly(lactic acid). The accomplishment of these objectives will contribute to study further property improvement of poly(lactic acid) film.

Table

Table 1

Energy required from non-renewable sources and CO_2 emissions for different types of plastics currently on the market

Type of plastic	Energy requirement, MJ/kg	Global warming, kg CO_2 eq/kg
From non-renewable sources		
HDPE	80.0	4.84
LDPE	80.6	5.04
Nylon 6	120.0	7.64
PET	77.0	4.93
PS	87.0	5.98
PVOH	102.0	2.70
PCL	83.0	3.10
From renewable sources		
TPS	25.4	1.14
TPS + 15% PVOH	24.9	1.73
TPS + 60% PCL	52.3	3.60
PLA	57.0	3.84
PHA	57.0	Not Available

References

Dash, T. K. and V. B. Konkimalla (2012). "Polymeric Modification and Its Implication in Drug Delivery: Poly-epsilon-caprolactone (PCL) as a Model Polymer." Molecular Pharmaceutics 9(9): 2365-2379.

Gironi, F. and V. Piemonte (2011). "Bioplastics and Petroleum-based Plastics: Strengths and Weaknesses." Energy Sources Part a-Recovery Utilization and Environmental Effects 33(21): 1949-1959.

Jamshidian, M., et al. (2010). "Poly-Lactic Acid: Production, Applications, Nanocomposites, and Release Studies." Comprehensive Reviews in Food Science and Food Safety 9(5): 552-571.

Kim, Y., et al. (2009). "Transparent nanocomposites prepared by incorporating microbial nanofibrils into poly(L-lactic acid)." Current Applied Physics 9: S69-S71.

Li, Y., et al. (2009). "Crystallization Improvement of Poly(L-lactide) Induced by Functionalized Multiwalled Carbon Nanotubes." Journal of Polymer Science Part B-Polymer Physics 47(3): 326-339.

Lv, R. T., et al. (2014). "Building Complex Hybrid Carbon Architectures by Covalent Interconnections: Graphene-Nanotube Hybrids and More." ACS Nano 8(5): 4061-4069.

Mohanty, A. K., et al. (2002). "Sustainable Bio-Composites from Renewable Resources: Opportunities and Challenges in the Green Materials World." Journal of Polymers and the Environment 10(1-2): 19-26.

Mohanty, A. K., et al. (2000). "Biofibres, biodegradable polymers and biocomposites: An overview." Macromolecular Materials and Engineering 276-277(1): 1-24.

Nakayama, N. and T. Hayashi (2007). "Preparation and characterization of poly(L-lactic acid)/TiO2 nanoparticle nanocomposite films with high transparency and efficient photodegradability." Polymer Degradation and Stability 92(7): 1255-1264.

Norazlina, H. and Y. Kamal (2015). "Graphene modifications in polylactic acid nanocomposites: a review." Polymer Bulletin 72(4): 931-961.

Patel, M. (2002). "Life cycle assessment of synthetic and biological polyesters." Proceedings of the International Symposium on Biological Polyesters, Munster, Germany,.

Scott, A. (2000). Chem. Week.

Wang, R., et al. (2011). "Fibrous nanocomposites of carbon nanotubes and graphene-oxide with synergetic mechanical and actuative performance." Chemical Communications 47(30): 8650-8652.

Yates, M. R. and C. Y. Barlow (2013). "Life cycle assessments of biodegradable, commercial biopolymers-A critical review." Resources Conservation and Recycling 78: 54-66

CHAPTER 2: REVIEW OF LITERATURES

Poly(lactic acid)

Discovery and Origin

Poly(lactic acid) was discovered by a DuPont scientist Wallace Caruthers in the 1930s and it was a form of low molecular weight. The first poly(lactic acid) was produced by heating lactic acid under vacuum. Due to the high cost of the polymer, initial poly(lactic acid) polymer was used only as medical grade such as sutures implants and controlled drug release applications. After all, Japanese companies such as Shimadzu and Mitsui Tuatsu have developed limited quantities of polylactic acid for more commercial grade plastics applications, but the high cost problem has not been solved (Garlotta 2001). In 1954, DuPont scientists developed synthesizing poly(lactic acid) by fermentation of corn which lowered the cost of production and increased the potential application of poly(lactic acid). In these days, Cargill Dow Polymers LLC which is now trading as NatureWorks LLC, owned the world largest production plant of poly(lactic acid) in Blair, Nebraska. Recently most of poly(lactic acid) is derived from renewable resources such as corn starch, tapioca roots, and sugarcane. Poly(lactic acid) is aliphatic polyesters usually made out of alpha-hydroxy acids. The basic unit of poly(lactic acid) is lactic acid which was discovered by Swedish chemist Scheele in 1780. Lactic acid was isolated from sour milk and produced commercially in 1881 (Singha and Thakur 2012). By then, majority of lactic acid was applied to food industry while it was also used as a buffering agent, bacterial inhibitor, and acidic flavoring agent. Before fermentation method dominated the production of lactic acid, it usually produced by chemical synthesis (Hartmann 1998).

Synthesis of Poly(lactic acid)

The single monomer of poly(lactic acid) is lactic acid which is also known as 2-hydroxy propionic acid and has two optical active configurations. D(-)-enantiomers and L(+)-enantiomers are both produced by bacterial fermentation of carbohydrates. There are homofermentive and heterofermentive activity of bacterial fermentation. Homofermentive is more favorable in industry production since the pathway has greater yield production of lactic acid and less production of by-products. As explained previously,

industrial production preferred the lactic fermentation process than chemical synthesis due to lower cost and less by product (Datta and Henry 2006). Bacterial fermentation of carbohydrates adapted homolactic organisms such as modified strains of genus *Lactobacilli* which form lactic acid (Hartmann 1998). Each isomer is yielded from many different *Lactobacilli* organisms. *Lactobacilli amylophilus, L.salivarius, L.bavaricus, L. casei, and L. maltaromicus* yield L(+)-isomer. L. delbrueckii, L. acidophilus and L. jensenii yield the D-isomer or mixture of both D and L-isomer. These bacteria are categorized as homofermentive activity using Embden-Meyerhof pathway and yield greater than 90% of lactic acid from glucose. These fermentation have desirable conditions to bring greatest yield which are pH range of 5.4 to 6.4, temperature range of 38 to 42 ^{o}C, and low oxygen concentration (Mehta R 2005). Each bacterial strain is restricted to certain available nutrients and carbohydrates. Besides carbohydrates, nutrients such as amino acids, nucleotides and B-viatmins are essential to yield poly(lactic acid). Usually soy flour, cottonseed flour and corn steep liquor contain these nutrients. Generally most of simple sugars, which can be obtained from agriculture byproducts, are considered as common carbohydrates. Lactose from cheese whey, glucose from corn, and sucrose form beet sugar are used as carbohydrates for *Lactobacilli* strain fermentation (Garlotta 2001).

Batch process is the common way in industry fermentation for poly(lactic acid) production. Due to toxicity and growth inhibition in the high concentration of sugar, many neutralization and extraction method have been introduced to achieve most efficiencies. To neutralized the fermentation acid, calcium hydroxide can be added to the batch. The mixture turns into soluble calcium lactate solutions. This calcium lactate solution is filtered to remove the cell biomass and goes under evaporation, recrystallization and acidifying with sulfuric acid. Calcium sulfate, which is made out of acidifying, can be removed by filter and discarded. Over multiple times of distillation of the acid, batch will obtain higher purity of lactic acid (G. B. Kharas 1994).

Figure 1. (Jamshidian, Tehrany et al. 2010) depicts the current high molecular weight poly(lactic acid) production methods. Recently Mitsui Toatsu Chemicals developed most efficient way to produce high molecular weight poly(lactic acid) using direct poly-condensation in an azeotropic solution with catalyst. This leads to obtain poly(lactic acid) with weight-average molecular weights higher than 300,000 (Ajioka, Enomoto et al. 1995). Before azeotropic solution was introduced to poly(lactic acid) production, there were

two different method to produce high molecular weight poly(lactic acid). As depicted in figure 2. (Lunt 1998), lactic acid undergoes condensation to become low molecular weight which is used as chain coupling agents to produce high molecular weight poly(lactic acid). The other pathway is that low molecular weight poly(lactic acid) undergoes depolymerization and collect lactide to yield high molecular weight poly(lactic acid). This lactide method is only way to produce high purity of high molecular weight poly(lactic acid) until Mitsui Toatsu Chemicals (Ajioka, Enomoto et al. 1995).

Condensation polymerization in figure 2 is the least expensive way for the production. However, since condensation is solvent free pathway, it is extremely hard to obtain higher molecular weight poly(lactic acid). Therefore, coupling agents or esterification-promoting adjuvents is introduced which unfortunately increased the cost of production (Inata and Matsumura 1985). For coupling agents, they react with different kinetic reaction rates based on either the hydroxyl or carboxyl group. Both hydroxyl terminated and carboxyl terminated poly(lactic acid) share same mechanism of chain coupling. Both achieve coupling by condensation of lactic acid in presence of hydroxyl compounds and carboxyl compounds. Furthermore, poly(lactic acid) can be predesigned for desirable terminating functional group by reacting with acid anhydrides which converts hydroxyl to carboxyl (Spinu, Jackson et al. 1996). Coupling agents method also has low cost of production since it only need low amount of coupling agents and no need for extra separation steps. On the other hand, final poly(lactic acid) is not as pure as esterification-promoting adjuvents method and extended chains might not be biodegradable (Hartmann 1998).

Esterification-promoting adjuvents is another way to increase the molecular weight of condensed poly(lactic acid) and dicyclohexylcarbodiimide and carbonyl diimidazole are great examples of it (Buchholz 1994). Esterification-promoting adjuvents produce highly purified final products while it increases costs due to increased number of reaction steps such as additional purification and separation steps for byproducts. Besides it uses hazardous solvents and is not able to make copolymer with different functional group (Hartmann 1998).

The azeotropic condensation polymerization method yields highest molecular weight polymers. However, this method needs solvents and residual catalyst, which can result impurity of final product. This residual catalyst can occur unwanted degradation, uncontrolled degradation rate, toxicity, and differing

slow release property in drug delivery. Residual catalyst can be removed by precipitation and filteration with strong acid (Garlotta 2001).

As shown in figure 2., lactide can be obtained from the depolymerization of low molecular weight poly(lactic acid). The ring-opening polymerization of lactide was first introduced in 1932 but higher molecular weight cannot be achieved until DuPont introducing purification method. Lactide purification has been achieved by using vacuum-distillation of high temperatures. After successful purification of lacitde, high molecular weight poly(lactic acid) can be obtained by using ring-opneing polymerization of lactide. It can be carried out in either cationic or anionic (Jamshidian, Tehrany et al. 2010). Additionally Lactide can be formed in three different way as L-lactide, D-lactide, and meso-lactide. The percentage of each form in mixture depends on temperature, catalyst and isomer feedstock (Garlotta 2001).

Both cationic and anionic formation usually is carried out in solvent. Due to its high reactivity in solvent, impurity and racemization become huge drawback of this mechanism. In large scale industry, it prefers to initiate the polymerization in bulk melt condition using nontoxic metal catalysts such as zinc, aluminum, tin etc. Furthermore, tin(II) oxide or octate has been found as greatest conversion which is greater than 90% and least racemization as a catalyst (Kricheldorf and Serra 1985). Nowadays, tin octate has been widely used in poly(lactic acid) polymerization due to its low toxicity and ability to produce high molecular weight polymers with low racemization.

Polymerization rate of poly(lactic acid) depends on followings: impurities, percent of amorphous phase in the polymer, and the addition of free hydroxylic or carboxylic acid (Braunecker and Matyjaszewski 2007). Addition of free carboxylic acid does not affect molecular weight but decreases polymerization rate since free acid reacts with catalyst reducing catalyst activity. On the other hand, addition of free hydroxylic acid presents opposite outcome. Hydroxylic impurities increase the rate of polymerization and affect final molecular weight by interacting with both lactide and catalyst such as tin(II) octate (Vanderweij 1980).

Physical Properties and Crystallization Behavior

Poly(lactic acid) has relatively high mechanical strength, low toxicity and relatively good barrier properties among other biodegradable polymers. Table 1. (Jamshidian, Tehrany et al. 2010) shows the

comparison of physical properties of poly(lactic acid) among other biodegradable polymers. Tensile strength of poly(lactic acid) is between 48 to 53 MPa which is higher than polystyrene but significantly lower than polyethylene terephthalate. Melting point (T_m) of poly(lactic acid) is around 130 to 180 ^oC and glass transition temperature (T_g) around 40 to 70 ^oC which is lower than polystyrene and polyethylene terephthalate. Low glass transition temperature (T_g) gives limit of usage in thermal related packaging. Poly(lactic acid) has highest tensile modulus among biodegradable polymers. For notched izod impact performed by Dorgan group shows that poly(lactic acid) presents lowest impact strength among common polymers (Dorgan, Lehermeier et al. 2000). Researcher group of Lalla and Chugh concluded that the degree of orientation and stereochemcial composition of poly(lactic acid) influence the physical properties shown in table 2 (J. K. Lalla 1990). Effect of stereochemistry and crystallinity on mechanical properties is shown in table 3. Annealed poly(lactic acid) demonstrated higher impact resistance and increased tensile strength compared to non-annealed one due to crosslinking effects of the crystalline domains and stereoregularity of the chain (J. K. Lalla 1990).

Table 3. (Jamshidian, Tehrany et al. 2010) shows the barrier property of poly(lactic acid). Researcher group of Lehermeier studied on poly(lactic acid) (L:D ratio 96:4) gas permeation properties: N_2 permeation was 1.3 (10^{-10} cm^3cm/cm^2scm Hg); O_2 permeation was 3.3 (10^{-10} cm^3cm/cm^2scm Hg); CO_2 permeation was 1.0 (10^{-10} cm^3cm/cm^2scm Hg) at 30 ^oC. The authors defined that small changes in L:D stereochemical content does not change permeation properties, but only depends on crystallinity of film (Lehermeier, Dorgan et al. 2001). On the other hand, researcher group of Bao disagreed with previous conclusion that stereochemcial content has significant impact on permeation properties. Bao group adopted time lag method to deteremine gas permeation, diffusivity and solubility. The results are following (98.7% L, 1.3%D): N_2 permeability, diffusivity and solubility are 0.05 (10^{-10} cm^3cm/cm^2scm Hg), 2.4 * $10^{-8}cm^2/s$ and 2.2 * $10^{-4}cm^3/cm^3cmHg$ respectively (Bao, Dorgan et al. 2006). Researcher group of Shogren reported that water vapor transmission rate of crystalline and amorphous poly(lactic acid) in 6, 25 and 49 ^oC as 27, 82, and 333 g/m^2 per day for the crystalline form and 54, 172, and 1100 g/m^2 per day for amorphous form respectively. It shows that not only crystallinity determines the water vapor transmission rate but also the temperature determines it (Shogren 1997). Furthermore, researcher group of Tsuji studied the influence of degree of crystallinity and molecular weight on water vapor transmission rate. The authors concluded that

more restricted amorphous region and higher molecular weight of poly(lactic acid) cause less water vapor transmission (Tsuji, Okino et al. 2006).

Poly(lactic acid) crystals have three different structural positions called alpha, beta and gamma. Different helix conformations and cell symmetries determine each structural position and ultimately affect the thermal and mechanical properties (Kawai, Rahman et al. 2007). The crystallization behavior of poly(lactic acid) is closely related to molecular weight and stereochemistry of backbone. Polymerization with D-lactide, L-lactide, D,L-lactide or meso-lactide determine the stereochemistry of poly(lactic acid). This is also able to control the degree of crystallinity and mechanical properties (Garlotta 2001). Furthermore, hydrolytic degradation of the polymer can be determine by the degree of crystallinity such as higher percent of amorphous polymer degraded faster than higher percent of crystalline polymer.

Thermal Stability

Poly(lactic acid) has poor thermal resistance due to various reasons during heat process such as random chain scission, depolymerization, oxidative degradation, intramolecular and intermolecular transesterifications hydrolysis, pyrolytic elimination and radical reactions (Carrasco, Pagès et al. 2010). Random chain scission reaction has been studied by group of Doi who concluded that thermal degradation occurred by random chain scission regardless of the type and chemical composition (Doi, Kanesawa et al. 1990). Intramolecular transesterification reactions and intermolecular transesterification are the major reasons of degradation of poly(lactic acid) during melt. They are either reaction between two ester molecules by exchanging radicals or process of exchanging the ester with an alcohol (Wachsen, Platkowski et al. 1997). Hydrolysis is cleaving ester linkage depending on the water content and gives characteristic of poly(lactic acid) thermal instability. Only on temperature above 250 ^{o}C, radical degradation is considered main reason of poor heat resistance (Kopinke, Remmler et al. 1996).

X-ray Diffraction (XRD)

X-ray diffraction obtains the structure of crystalline materials. It is beneficial analysis since it can test compounds in various forms such as powder, film and samples will be undamaged after test. The technique is identifying and characterizing compounds based on the diffraction pattern. The process of

diffraction can be defined as constructive and destructive interference of scattered X-rays. The X-rays are projected by cathode ray tube, but only produces monochromatic radiation. These X-rays are than collimated to concentrate and delivered directly toward sample. Once X-rays hit an atom, it makes the electronic cloud move with atom's own frequency. The movement of electronic cloud emitting the same frequency and intensity and angle of this frequency are measured. The X-ray diffraction is described by Bragg's Law which is $n\lambda = 2d\sin(\Theta)$. A diffraction pattern is obtained by intensity of scattered waves as a function of scattering angle. Once scattering angles meet the Bragg condition, Bragg peaks which is strong intensity can be obtained. In addition to above, X-ray diffraction can quantify the percent crystallinity of sample. Commercialized poly(lactic acid) (L:D = 96:4) has intense peak at $2\Theta = 16.6^{o}$. Other smaller peaks are also found near at 14.8, 20.0 and 22.2^{o} (Carrasco, Dionisi et al. 2006).

Differential Scanning Calorimetry (DSC)

Differential scanning calorimetry determines followings during heating and cooling process: (i) melting point (T_m) of compound; (ii) stability of the compound; (iii) relative stability of different crystalline forms; (iv) crystallization behavior after heating; (v) thermal transition. Differential scanning calorimetry measures the amount of heat energy absorbed or released during heating and cooling process. If any type of transitions occurs during this process, the measured temperature will be different to a reference sample. Figure 4. shows the typical commercial poly(lactic acid) differential scanning calorimetry curve. Melting point (T_m) of poly(lactic acid) is between 130 and 180 ^{o}C. Glass transition temperature (T_g) is usually between 40 and 70 ^{o}C. Differential scanning calorimetry also can measure cold crystallization enthalpy (ΔH_c) and melting enthalpy (ΔH_m) in Jg^{-1}. Furthermore, using equation $\chi_c\,(\%) = 100 \times (\Delta H_c + \Delta H_m)/\Delta H_{mc}$ percent crystallinity of compounds can be calculated where ΔH_{mc} is enthalpy of 100% crystalline (93.6 Jg^{-1}) (Pinto, Cabral et al. 2013).

Mechanical Test

There are list of mechanical properties and their description following:

(a) Tensile strength (MPa): It is the ability of a material to withhold a vertically pulling force. This measurement is critical in material science especially on brittle materials more than

ductile materials. The maximum stress is measured right before material is deformed or stretched. Typically biodegradable polymer shows both pattern of failure. While measuring tensile strength, either ductile failure or brittle failure can be observed. Ductile failure has first and second failure and represents neck formation while brittle failure only exhibits single breaking point. Commercial poly(lactic acid) has around 59MPa of tensile strength measured followed by American Society for Testing and Materials (ASTM).

(b) Elongation at break (%): It is also called as fracture strain that defined by ratio of changed length and initial length after breakage of material. It defines the capability of a material to resist the changes of shape until complete breakage. Commercial poly(lactic acid) has around 7.0% of elongation at break.

(c) Modulus of elasticity (Mpa): It is also called as Young's modulus (E). Young's modulus describe the stiffness of material. It is a mathematical term that slope of stress vs strain curve. Following equation can be adapted for E:

λ = stress / strain ; λ (E, MPa); Stress (MPa); Strain (unitless)

Modulus of elasticity is also shown in figure 5.

(d) Yield strength (Mpa): It is the stress beyond which a material becomes plastic. Commercial poly(lactic acid) has around 70 MPa of yield strength.

(e) Notched izod impact (J/m): It is the energy needed to break notched material under standard condition. Notched izod impact cannot be considered as an indicator of overall toughness of material. Commerical poly(lactic acid) has around 26 J/m of impact energy.

Mechanical test of biodegradable polymer must be followed by ASTM D3039 (Standard Test Method for Tensile Properties of Polymer Matrix Composite Materials). ASTM D3039 illustrated followings: rectangular cross section specimen with greater than 2mm x 3mm (gauge width x gauge length), specimen conditioned in 55% humidity and room temperature for 48 hours, and test speeds around 2 mm/min.

Oxygen Transmission Rate (OTR)

Oxygen transmission rate (OTR) is the volume or amount of oxygen gas passing through specimen over a certain time. The unit for oxygen transmission rate is $cm^3*cm/cm^2*s*cmHg$. This is the most important factor on food packaging industry due to contamination of food. Researcher group of Lehermeier had measured oxygen transmission rate based on different ratio of L:D (96:4 and 98:2) stereochemistry and at different temperature. The authors concluded that the ratio of L:D did not affect the oxygen transmission rate. However, researcher group of Bao suggested that the L:D ratio is strongly effective to oxygen transmission rate shown in table 4 (Bao, Dorgan et al. 2006). Besides, oxygen transmission rate is directly related to temperature shown in figure 6 (Lehermeier, Dorgan et al. 2001).

Scanning Electron Microscope (SEM)

Scanning electron microscope releases a focused beam of electrons carrying significant amounts of kinetic energy. Once high-energy electrons reach to material, the energy produces variable signal to deliver morphology, chemical composition and crystalline structure. The data is collected as 2-dimensional image with magnification ranging of 20X to 30,000X and spatial resolution of 50 to 100nm. Scanning electron microscope is also beneficial to distinguish phases based on atomic number. Furthermore, it has precise measurement of nano-scale in size (Yoshimura 2014). However, there are few conditions for materials to be successfully imaged: (i) non-volatile, (ii) free of contaminants, (iii) able to withstand electron beam irradiation, (iv) produce atomic based contrast, (v) thin enough for electron transmission (vi) prepared for vacuum environment. To achieve best image of materials, ultramicrotome is often suggested (Schrand 2005).

Energy Dispersive X-ray Spectrometry (EDS)

Once focused electron beam hit a solid sample, it emits X-ray spectrum which EDS can have a localized chemical analysis. X-ray results vacancy of inner orbit (normally inner orbits are full) so that electron transitions are detected by electron probe to identify a specific atom (Reed 1993). EDS can detect all elements from atomic number 4 to 92 by reading a specific energy of photons (X-ray). Qualitative (identifying the lines in the spectrum) and quantitative (concentrations of the elements) analysis are

performed collaboratively to project element distribution images (B.K. 1991). This images or maps have X-ray energy in x-axis (in cahnnels 10 or 20 eV wide) and number of counts per channel in y-axis. Usually the scanning electron microscope (SEM) can perform EDS analysis if an X-ray spectrometer is equipped. The overall accuracy of EDS is generally ±2%, which is relatively accurate. Sample must be a vacuum compatible material, well polished due to influence of surface roughness, any size and shape, placed on rectangular glass slides, electrically non-conducting, and coated with conducting surface (Russ 1984).

Light Emission Test

Transparency and ultraviolet B radiation (UVB light) blockage are key factors in food packaging industry. Visible light has wavelength around 500nm and UVB light wavelength is between 320nm and 290nm. Packaged food, which has been exposed to UVB light often undergoes food degradation. Commercial poly(lactic acid) only prevents 40% of UVB light which is not suitable for food packaging material. However, it has great transparency transmittance around 75%, which is comparable to petroleum based plastics. Most common method to measure the amount of light material absorb is a spectrophotometer. Stream of photons, emitted by spectrophotometer, is absorbed by analyte in material. The reduced amount of photons in the beam of light reduces the intensity of light (Valapa, Pugazhenthi et al. 2015).

Poly(lactic acid) Processing Technologies

Commercial poly(lactic acid) is in a form of either semicrystalline resins or amorphous resins. Based on different types and characteristics of resins, different processing technologies have to be adopted. Also based on specific packaging demands, different approach of processing is needed. Since poly(lactic acid) is sensitive to humidity and temperature, to minimize the degradation of products, the resins have to be preconditioned and dried. Usually poly(lactic acid) resins are packaged with 0.04% w/w moisture content and drying is essential before processing to final product. Desirable drying condition is at 80 ^{o}C for 4 hours and kept in vacuum until usage.

Following are processing technologies and table 5 shows adequate process technologies among each polymer:

(i) Extrusion: It is the most common way to convert solid polymer to liquid phase. Screw extruders are well known industry techniques which consist of electrically heated metal barrel, motor for screw, a hopper for resin feeding, and a die where melted polymer exists. The screw with larger L/D ratio (flight length of screw/screw's outer diameter) produces better mixing and higher shear heating (Giles FH 2005).

(ii) Injection molding: It is similar to extrusion in the way involving melting a thermoplastic. However unlike extrusion, reciprocating screw both rotates and moves forward and backward during cycle. Recommended compression ratios are 2.5 to 3 at melting temperature 200 to 205 ^{o}C. Majority of commercial polymers are adequate to use this techniques (Jamshidian, Tehrany et al. 2010).

(iii) Blow molding: Chilled mold is conformed by blowing up a hot thermoplastics tube. Blow molding has three common methods:

a. Extrusion blow molding: Extrusion of polymer → chilled mold isolated → blowing air to form the shape → cooling process

b. Injection blow molding: It is desirable method for large volume of production of small parts with precise quality dimensions. It has unique molded parison called preform. Preform is advantageous on producing precise dimensions and detail in finish than extrusion blow molding.

c. Injection stretch blow molding: It has two modification of injection blow molding which are shorter preform and a stretch rod (Jamshidian, Tehrany et al. 2010).

(iv) Cast film extrusion: Extrusion of polymer → high speed rolls → chrome-plated and water-cooled → solidification of products with chill roll

It has advantages on fast production, ability to control thickness, uniformity and good transparency (Giles FH 2005).

(v) Thermoforming: It draws and presses pliable plastics into final shape by air pressure. It is most common technique in food packaging industry.

Food Packaging Application

Poly(lactic acid) is one of the most promising biodegradable polymer. It is a growing new "green" food packaging polymer that is renewable, sustainable and price competitive among other biodegradable polymers. 70 percentage of poly(lactic acid) application is in packaging nowadays. Table 5. shows increasing poly(lactic acid) market and future potential market. Furthermore it has unique barrier properties, low temperature heat sealability and great transparency. Ideally poly(lactic acid) is suitable on fresh food products and short term packagings due to its barrier properties and aroma barrier characteristics (Jamshidian, Tehrany et al. 2010). However, poly(lactic acid) needs higher temperature for complete degradation by hydrolysis compared to other biodegradable polymers which is necessary to be studied as food packaging (Siracusa, Rocculi et al. 2008). In addition to, commercial poly(lactic acid) is usually semicrystalline, high molecular weight, and has water solubility resistance. Water bottle, food tray, and bowls for fast food are possible applications. For the last, poly(lactic acid) has promising material in release studies. Unlike old packaging technique such as extending shelf-life of food, release studies introduce new aspect of improving food packaging. Poly(lactic acid) has great potential to carry out as an active packaging such as antioxidants release, carrying CO2 scavengers and moisture regulators (Lopez-Rubio, Almenar et al. 2004).

Antimicrobial packaging becomes growing interest as well as active packaging agent. For last decade, many researchers have approached to develop slow release of antimicrobial with poly(lactic acid) (Jin, Liu et al. 2009). Even if variable active additives exist such as nisin, it is still a huge challenge to successfully control release active agents in desirable rate and desirable amount. Recently mathematical modeling of active agent-controlled release (Pocas, Oliveira et al. 2008) and monitoring active agent desorption from a multi-layer polymer film (Chollet, Swesi et al. 2009) have been studied.

Graphene, Graphene Oxide and Carbon Nanotube

Discovery and Origin

Graphene is the fewest layer of graphite. Geim and others first observed single layer of graphene at Manchester University in 2004. However graphene is very common resources because it has been used widely. For example, graphite has been used as crude mineral since 500 years ago and has been part of pencils in these days (Allen, Tung et al. 2010). Before single layer of graphene was observed, it has been discussed since 1947. According to Landau and Peierls, grephene was thermodynamically unstable two-dimensional crystals. Without compromising with three-dimensional crystals, graphene theoretically cannot be free state (Peierls 1935). Later group of scientists presented supportive experiment. They observed films become thermodynamically unstable while melting temperature decreases with decreasing thicnkness of thin film (Mermin 1968). However, this thin film is still consisted of dozen of atomic layers which cannot be considered as single layer of graphene. Recent discovery by Geim revised the theory of two-dimensional crystals and defined zero to three-dimensional crystals.

Nowadays, throughout tons of research, it became clear to define two-dimensional crystals that number of single layer have to be under ten single layers (Partoens and Peeters 2006). A single layer, two single layers and more than three single layers (<10 layers) can be distinguished as three different type of two-dimensional crystals by electronic spectra. Bilayer (two single layer) exhibits only simple electronic spectra which is zero-gap semiconductors (Geim and Novoselov 2007).

Isolation of Graphene

Figure 7. is the image of single layer of graphene (Novoselov, Geim et al. 2005). Micromechanical cleavage of bulk graphite is the first graphene isolation method. Repeated peeling of graphite with adhesive tape, followed by micro-cleavage, is well known technique to obtain graphene (Novoselov, Jiang et al. 2005). The adhesive tape is pressed down again the substrate to deposite graphene and graphite flakes. Due to van der Waals force, graphene relatively bonds and remains on substrate while graphite flakes are removed with the tape. With appropriate skill of the isolating process, this technique provides high quality crystallites in around 100 μm^2 size (Novoselov, Jiang et al. 2005).

Researchers have tried mechanical exfoliation to isolate graphene. Ruoff's group adopted an atomic force microscope tip to create small pillar patterned of pyrolytic graphite by plasma etching. The thinnest layer had been found was around 600 layres. Kim's group at Columbia and Enoki's in Tokyo also attempted to improve mechanical exfoliation by transferring pillars to a tipless cantilever and using 1600^{o}C heat to convert nanodiamonds into graphene respectively (Allen, Tung et al. 2010). While many other isolation methods have been proposed, they only obtained 20 to 100 layers thick of graphene flakes. Graphene crystallites are usually hidden between haystack of thick graphite flakes. Even if it was successfully micro-cleavage, it is hard to locate the graphene crystallites. After all, Si wafer has been introduced to enhance visual observation of graphene layer. Graphene on the Si wafer gives visibility in an optical microscope, but there are many restriction such as precise thickness of SiO_2. Other two-dimensional crystals (monolayer) have also never been isolated to study the properties (Geim and Novoselov 2007).

Chemical exfoliation is the earliest attempt to isolate graphene. Bulk graphite was first intercalated to separate graphene planes by layers of intervening atoms or molecules (Dresselhaus and Dresselhaus 2002). However, this method usually ends up isolating three-dimensional graphene. Unfortunately this chemical reaction can cause restacked graphene sheets due to intervening molecules removal. In addition to chemical exfoliation, researchers attempted to grow carbon nanotube and grapehen with variable method such as chemical vapor deposition (CVD) of hydrocarbons on metallic substrate to isolate graphene (Land, Michely et al. 1992).

Recently, Hassan et al. introduced high yield aqueous phase exfoliation of graphene for facile nanocomposite synthesis via emulsion polymerization using expanded graphite (Hassan, Reddy et al. 2013). Prepared thermal expanded graphite is dispersed in 20 mL distilled water by mixing 0.1 wt% expanded graphite with variable amounts of sodium dodecyl sulfate as surfactant and stabilizing agent. The mixture undergoes sonication process and continued in situ emulsion polymerization to synthesize poly(styrene)-graphene nanocomposite. By centrifugation, graphene can be separated with non-exfoliated graphite. The yield of less than 5 layer graphene was 60% considered as high yield production (Hassan, Reddy et al. 2013).

General outline of Graphene-based materials

Graphite is made of many layers of graphene. Graphene sheets stack with an interplanar spacing of 0.335 nm to form graphite. It is naturally a very brittle compound but has great advantages: (i) electric conductivity, (ii) heat conductivity, (iii) high resistance to chemical attack, (iv) self lubricating etc. Graphite is one of the three naturally occurring allotropes of carbon among diamond and amorphous carbon (Norazlina and Kamal 2015).

Graphene is a two-dimensional sheet of sp^2-hybridized carbon. It is a single layer of carbon atoms bonded together in a hexagonal lattice or also called honeycomb network (Geim and Novoselov 2007). It is also described as an atomically thin layer of carbon. Graphene is the basic structure of other allotropes to form zero-dimensional fullerenes, rolled into one-dimensional nanotubes or stacked together into three-dimensional graphite (figure 8). Graphene has been known as one of the strongest materials (a breaking strength over 100 times greater than steel) with stiffness 1,000 MPa (Li, Kudin et al. 2006). Followings are benefits of single layer of graphene (Suk, Piner et al. 2010):

(i) Fracture strength is 130 GPa.

(ii) It has ~5,000 W/mK thermal conductivity.

(iii) Electrical conductivity is10^4 S/cm.

(iv) Thermal conductivity is significantly higher than graphene oxide (~2,000 W/mK), multiwalled carbon nanotubes (~3,000 W/mk), and single-wall carbon nanotubes (~3,500 W/mK).

(v) It has excellent electric charge transport.

(vi) It has 97.7% optical transmittance

(vii) High light transmittance, photoluminescence, and high charge mobility are presented.

Structural Features of Graphene Oxide

The exact chemical structure of graphene oxide has been raised as debate over the years. Graphene oxide is such a complex material because of amorphous, nonstoichiometric atomic composition, and lack of analytical techniques to characterize this material. However, there are considerable structures suggested shown in figure 9 (Dreyer, Park et al. 2010).

The first structural models of grapehen oxide was suggested by Hofmann and Holst. It was regular lattices composed of repeat units. It consists of epoxy groups distributed around graphite plane (sp^2 hybridization) and has a net molecular formula of C_2O (Hofmann and Holst 1939). Ruess proposed a model consist of hydroxyl groups into the graphite plane accounting for the hydrogen content of graphene oxide. The graphite plane in Ruess' model, unlike Hofmann and Holst, has sp^3 hybridization with a repeat unit. He suggested that only ¼ of cyclohexanes have epoxides in the 1,3 positions and hydroxyl groups located in 4 position (Ruess 1946). Scholz and Boehm proposed a model replacing epoxide and ether groups with regular quinoidal species in a corrugated backbone in 1969 (Scholz and Boehm 1969). The most recent model proposed by Lerf and Klinowski disagreed with lattice graphite plane. Instead, this model is based on nonstoichiometric and amorphous alternatives (Lerf, He et al. 1998).

Characterization of Graphene Flakes

Using optical microscope is good way to locate thin graphite flake, but cannot identify sinlge, double or multilayer of graphene. Identifying thickness of graphene layer is important since the thickness determines the characteristics of graphene. Scanning probe microscopy and atomic force microscopy are common way to determine the thickness of crystallite. Single layer of graphene is typically around 0.6 to 1.0nm (Novoselov, Falko et al. 2012). Unlike scanning probe microscopy, Raman spectroscopy is more useful and reliable to measure the thickness of mechanical exfoliated flakes. Raman spectroscopy observes the gradual change of electronic structure by stacking of successive layers of either graphene or graphite flake (Allen, Fowler et al. 2008). There are major features of the Raman spectra as following:

(i) G band at ~1584 cm^{-1} and G' band at ~2700 cm^{-1}.

The change of position and peak height of G and G' band indicates the number of layers of graphite flask.

(ii) Single layer: location of G peak is at 3-5cm^{-1} / peak height remains same
G' band as a single sharp peak at lower shift/ 4 times of G peak height

(iii) Bulk graphite: location of G peak is higher than 5cm^{-1} / peak height remains same
(Gupta, Chen et al. 2006).

Synthesis of Graphene Oxide and Conversion of Graphite

Producing high quality of graphene oxide (GO) has been always challenging even if there are numerous methods introduced. Grapehen oxide is manipulated graphite that chemically similar but structurally different with graphite oxide. Interplanar spacing between the individual graphene layer of graphene oxide is caused by water intercalation unlike graphite oxide. Another major difference is that graphene oxide is two-dimensional while graphite oxide is three-dimensional. However, they both have disrupted sp^2 bonding network due to oxidation process, they are potentially great electrical insulators (Norazlina and Kamal 2015).

The most common way to synthesize graphene oxide from graphite is Hummers and Offeman methods (Hummers and Offeman 1958). Hummers method is following:

(i) Add H_2SO_4 to graphite in three neck flask cooled in ice bath and stir for 15 minutes at under 5 ^oC

(ii) Slowly add $KMnO_4$ over 15 minutes, heated to 35 ^oC and leave the reaction for 24 hours

(iii) Add HCl to remove excessive $KMnO_4$ and add distilled water

(iv) Add excess aqueous H_2O_2 until bubbles observed and color changed to bright yellow

(v) Secure the sediments and wash them with distilled water until pH becomes 7

(vi) Brown powder (crude graphene oxide) can be obtained by freezing dryer

Instead of mechanical stirring to produce graphene oxide from graphite oxide, sonication is great alternative way in exfoliating graphite oxide (Chen, Zhu et al. 2010). Recently researcher has done minor modification on Hummers method to higher yield.

Reduced graphene oxide (rGO) is usually synthesized from graphene oxide. Treating graphene oxdie with hydrazine, and sodium borohydrate, graphene oxide can be reduced (Pei and Cheng 2012). Sodium borohydrate has been proved to be more effective on dehydration process of graphene oxide than hydrazine. Also using 98% H_2SO_4 at 180 oC after reduction by sodium borohydrate improves the dehydration process (Gao, Liu et al. 2010). Due to reduction, reduced graphene oxide is less hydrophilic than graphene oxide. There are few more effective method of producing reduced garphene oxide as following:

(i) Using ascorbic acid (vitamin C) as a substitute to hydrazine in the reduction of graphene oxide. This is a non-hazardous and non-toxic method (Fernandez-Merino, Guardia et al. 2010).

(ii) Photothermal reduction method exfoliates graphene oxide to reduced graphene oxide with highly porous which has better performance as the anode material (Guo, Peng et al. 2013).

(iii) UV irradiation conducts reduction of graphene oxide in titanium dioxide suspensions. Reduced graphene oxide becomes well exfoliated semiconductor composite (Williams and Kamat 2009)

(iv) Reduction of graphene oxide in ethanol interaction with excited zinc oxide nanoparticles. This method is the most cost efficient way (Williams and Kamat 2009).

(v) Urea can be an expansion reduction agent to synthesize graphene from graphite oxide. Heat applied to mixture of graphite oxide and urea which release reducing gases. The mixture is heated in an inert gas environment for short time. Solid graphene can be collected upon cooling cycle (Jin, Fu et al. 2013).

Graphene nanoribbons can be synthesized by unzipping multiwalled carbon nanotube (MWCNTs). There are five common unzipping techniques (Terrones, Botello-Mendez et al. 2010):

(i) Intercalation and exfoliation of multiwalled carbon nanotube with treating in liquid NH3 and Li followed by HCL and heat treatments respectively.

(ii) Strong acid treatment to break carbon-carbon bonds followed by oxidation by $KMnO_4$.

(iii) Catalytic approach, which metal nanoparticles cut the multiwalled carbon nanotube longitudinally.

(iv) Using electric current through multiwalled carbon nanotube

(v) Embedding multiwalled carbon nanotube into polymer and Ar plasma treatment

Recently, supercritical fluids (SCFs) process has been introduced to graphene to obtain high quality of graphene nano sheet in large-scale production. Without complicated steps of oxidation, chemical exfoliation and reduction process, supercritical O_2 process has succeed to intercalate and exfoliate layered

graphite. As a result, high quality few layer graphene (less than 10 layers) was obtained (Pu, Wang et al. 2009).

Complex Hybrid Graphene/Carbon Nanotube Structure

The most two common graphene synthesis are the reduction of graphene oxide and chemical vapor deposition (CVD). Graphene synthesized through reduction process tend to aggregate (stack together) to form layered structures in a dry state. Chemical vapor deposition tend to produce graphene with lower mechanical strength due to polycrystalline. To solve this problems, researchers suggest building a hybrid graphite nanostructure by covalent interconnection (Lv, Cruz-Silva et al. 2014). They assumed this hybrid nanostructure has not only solved problem but also enhanced the electronic transport, thermal transport and hydrogen storage properties. Here are three proposed hybrid nanostructures;

(i) Graphene-carbon nanotube hybrids

a. Carbon nanotube rich hybrid: graphene layers attached on the outer walls or inner cores of carbon nanotube. Outer wall of carbon nanotube can be partially unzipped and creat loos graphene layers. This hybrid has excellent oxygen reduction electrocatalyst.

b. Graphene rich hybrid: carbon nanotube can either vertically or horizontally attached to the surface of graphene layer. This prevents the graphene layer stacking. To synthesize vertical alignment of carbon nanotube, metal catalyst such as Co and Fe are necessary. Vertical alignment of carbon nanotube increases the porosity of hybrid nanostructure. Horizontally spread carbon nanotube is beneficial on high mechanical robustness and excellent field emission properties.

(ii) Three dimensional covalent carbon nanotube networks

a. Carbon nanotube is only building block to build three dimensional structure.

b. Covalent interconnection among carbon nanotube can be achieved by chemical and physical treatment such as template-assisted routes, electron beam irradiation processes, atomic welders etc.

c. It has great potential to be applied in electronics, bioapplication devices, strain gauge, oil absorption applications etc.

(iii) Three dimensional graphene networks

a. It is also known as graphene hydorgels, graphene foams, and graphene sponges.

b. Due to large-scale production and cost efficiency, reduction process is mainly adopted to synthesis this networks.

c. The networks have high porosity, good flexibility, high elasticity, light weight, high surface area, superhydrophobicity etc.

Applications of Graphene-based nanomaterials

In 2008, graphene started produced by exfoliation procedures to be scaled up in large quantities so that reduced the cost for consumers (Segal 2009). This has changed the entire landscape of application by reaching to various industries. These followings are potential application area of graphene :

(i) Biomedical area (delocalized surface π electrons can be used for drug delivery) (Goenka, Sant et al. 2014)

(ii) Gene therapy (graphene can reduce cytotoxicity and increase cell selectivity to successfully deliver cationic polymers or drugs) (Shen, Zhang et al. 2012)

(iii) Electric circuits and nanoelectronics

(iv) Chemical and industrial processes

(v) Composite mateirals

(vi) Energy technology (energy capcity)

(vii) Sensors

(viii) Catalysis

Most of the current interest of graphene application is in computer electronics. The idea about graphene replacing Si in electronic industries has been discussed. Furthermore, recent research on modification of biodegradable polymer with graphene has been drastically increased due to graphene's outstanding mechanical properties.

Incorporation Methods of PLA/Grapehe-based Nanomaterials

The incorporation of nanostructure into polymer matrix has been studied for last decade. The great challenging of incorporation is successful dispersion of nanostructure. Graphene-based nanomaterials including carbon nanotube and graphene oxide have tendency to stack or coagulate together (Roy, Sengupta et al. 2012). Polarity, molecular weight, hydrophobicity or reactive groups have to be considered to prepare the nanocomposite. There are three main strategies of nanocomposite;

(i) Solution interaction: Both polymer and graphene-based nanomaterials dissolved in solvent either itself or in the same solvent. Colloidal suspensions of graphene-based nanomaterials and polymer occurs by mechanical stirring or shear mixing. This is the easiest technique to incorporate nanocomposite, but solvent removal is the biggest limitation. Suggested solvents for graphene-based nanomaterials are water, acetone, chloroform, toluene, and dimethyl formamide which least cause stacking problem. Ultrasonication and bath sonic are often conducted for better dispersion. Researcher group of Cao prepared lyophilized graphene nanosheets with poly(lactic acid) in dimethylformamide solvent with sonication. It was conducted to compare the dispersion with graphene nanosheets in vacuum-filtered (Cao, Feng et al. 2010).

(ii) In situ intercalative polymerization: Graphene-based nanomaterials are dispersed in monomer solution and polymerization occurs. Unlike solution interaction, this process does not acquire pre-exfoliation of graphite and allows great dispersion of graphene layers. Graphene oxide also can achieve the great dispersion in monomer solution by this process. Both covalent and non-covalent bond between functionalized sheet (graphene etc.) and polymer matrix are available. Disadvantage of this process is complexitiy of process due to polymerization. In addition to, this method requires monomer units. Researcher group of Yang prepared poly(lactic acid) and thermally reduced graphene oxide composites by in situ intercalative polymerization. Author concluded that great dispersion of reduced graphene oxide in poly(lactic acid) matrix and great interfacial interaction were achieved (Yang, Lin et al. 2012) .

(iii) Melt intercalation: Graphene-based nanomaterials mix with polymer in heated molten state. It is usually processed in twin-screw extruder for larger scale of production. This process must avoid toxic solvent. This process exhibits poor dispersion of graphene-based nanomaterials since the large ratio of surfaces of graphene sheets to their thickness. Van der Waals forces interconnect each sheets of graphene and aggregation occurs. To solve the aggregation problem, Lei et al. proposed coating graphene with nanofilms of polymers (admicellar polymerization), which prevents the Van der Waals forces among graphene sheets (Lei, Qiu et al. 2012).

Poly(lactic acid)/Grapehene-based Nanocomposites

Interest of graphene oxide in nanotechnology has been increased due to its excellent electronic, thermal, and mechanical properties. Oxygenated surface of graphene oxide provide great dispersion in aqueous and organic solutions by electrostatic repulsion (Loh, Bao et al. 2010). These characteristics increase the research interest on fabrication of nanocomposites with biodegradable polymers.

Comparison between poly(lactic acid)/exfoliated graphite nanocomposites and poly(lactic acid)/micron-sized natural graphite composites has been conducted (Kim and Jeong 2010). X-ray diffraction and scanning electron microscope image show that exfoliated graphite exhibited homogeneous dispersion in poly(lactic acid) matrix with thickness of 15nm while aggregation was observed in micron-sized natural graphite composites. Young's modulus and thermal degradation increased significantly with graphene content up to 3 wt% for exfoliated graphite composites while there was no significant effect found in micron-sized natural graphite composites.

Murariu et al. prepared nanocomposite with poly(lactic acid) and expanded graphite. Even though there is no polydispersity index change found in addition of expanded graphite, the average molecular weight has been decreased with increasing wt% of expanded graphite. Expanded graphite increased the impurities of poly(lactic acid) initiating degradation during melt blending. Expanded graphite has been proved to be a great thermal retardant. Increasing wt% of expanded graphite extended temperatures for 5 or 50 wt% loss compared to that of neat poly(lactic acid). Authors assumed that expanded graphite increased diffusion pathway of the degradation of volatile decomposition products. As addition of expanded graphite,

crystallinity increased. However after 6 wt% of expanded graphite, crystallinity suddenly decreased due to poor dispersion. Expanded graphite also improved the Young's modulus and storage modulus compared to neat poly(lactic acid) (M. Murariu 2010).

Further research on poly(lactic acid)/expanded graphite nanocomposite has been performed by Hassouna et al. 3 wt% of nanocomposites were prepared by different rotor speed and time of melt blending. Authors concluded that change of the average molecular weight depends on the impurities present in expanded graphite and the processing conditions, but not the wt% of expanded graphite. Expanded graphite dispersion in poly(lactic acid) matrix can be improved by increasing screw speed and residence time of twin-screw extruder. Scanning electron microscope image confirmed the relationship between screw speed and dispersion. Raman spectroscopy was adopted to observe π states of carbon layers. The G and 2D band of expanded graphite nanocomposite were shited upward which indicates the increase of interaction between carbon layers. As the screw speed increased, the intensities of G and 2D bands of nanomcomposite decreased. It indicates less interaction occurred resulting better dispersion. Raman spectroscopy proved the relationship between screw speed and dispersion of expanded graphite (Hassouna, Laachachi et al. 2011).

Vacuum-filtered graphene nanosheets and lyophilized graphene nanosheets are prepared to compare the dispersion, morphology and properties. Vacuum-filtered graphene nanosheets exhibited poor dispersion in dimethylformamide due to Van der Waals forces between graphene nanosheets while other exhibits great dispersion in organic solvents such as dimethylformamide due to decreased Van der Waals forces. FESEM analysis confirmed the graphene nanosheets are homogeneously dispersed and no aggregation found. Thermal stability was improved as the addition of 2 wt% graphene nanosheets due to tortuous path effect which graphene nanosheets delayed the oxygen permeation and escape of volatile degradation products. Tensile strength and Young's modulus increased as 26% and 18% respectively at 0.2 wt% graphene nanosheets due to flake-like morphology of poly(lactic acid) and graphene nanosheets (Cao, Feng et al. 2010)

Poly(D,L-lactic-co-glycolic acid) (PLGA)/graphene oxide(GO) nanocomposite was prepared to study the effect of graphene oxide loading on thermomechanical and surface chemical properties. The average diameter of the nanocomposite nanofibers was lower than the neat PLGA fibers indicating that abundant negative charge on surfaces causing strong electrostatic repulsion in solution jet. The tensile

modulus of 1 wt% and 2 wt% of nanocomposites are 172.8% and 204.9% respectively higher than neat PLGA. Due to hydrogen boding and dispersion of graphene oxide nanosheets caused strong interfacial interaction between polymer matrix and nanomaterials (Yoon, Jung et al. 2011).

Poly(L-lactic acid) (PLLA)/graphene oxide (GO) nanocomposites with different graphene oxide wt% was prepared. Non-isothermal melt crystallization peak temperature was higher than neat PLLA. Crystallization peak temperature of 0.5, 1 and 2 wt% were around 97.0, 100.4, and 96.0 ^{o}C which are higher than neat PLLA. Isothermal melt crystallization peak temperature exhibited similar pattern with crystallization peak temperature. This DSC indicated that both iso and non-isothermal melt crystallization kinetics are improved indicating that graphene oxide can act as a nucleating agent for crystallization of PLLA (Wang and Qiu 2011). Similar research has been done that both carbon nanotube and graphene improved the crystallization behavior of PLLA. Here, carbon nanotube has stronger impact on crystallization behavior than graphene (Xu, Chen et al. 2010).

Tables and Figures

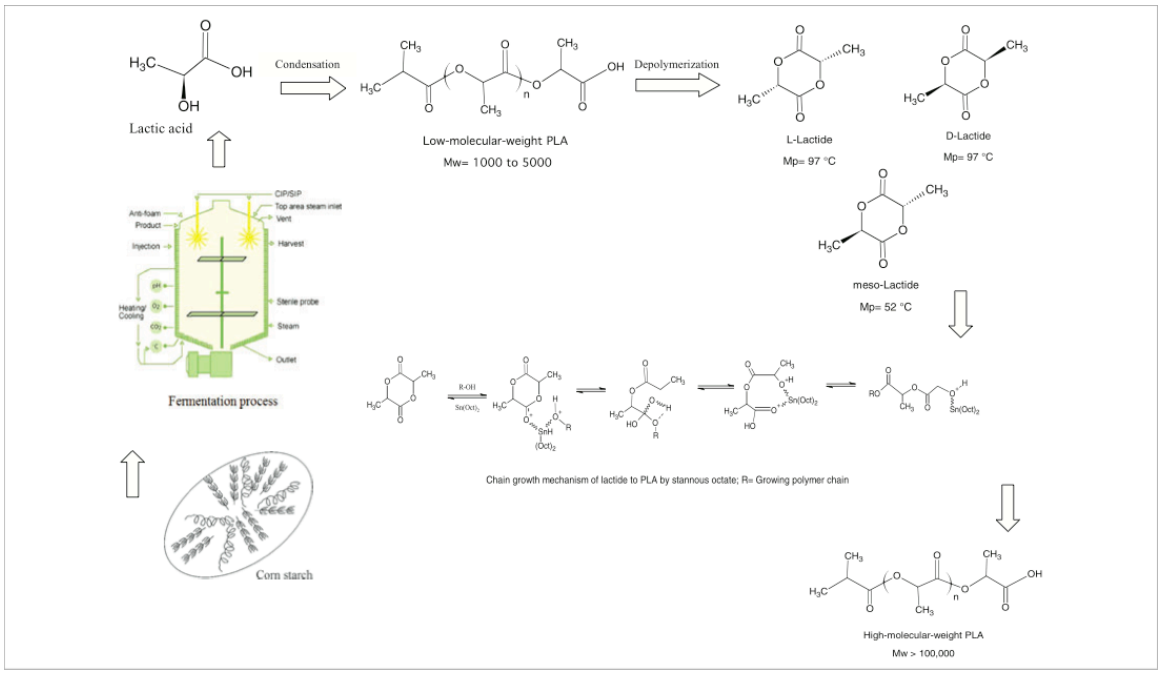

Figure 1. Synthesis methods for current poly(lactic acid) production.

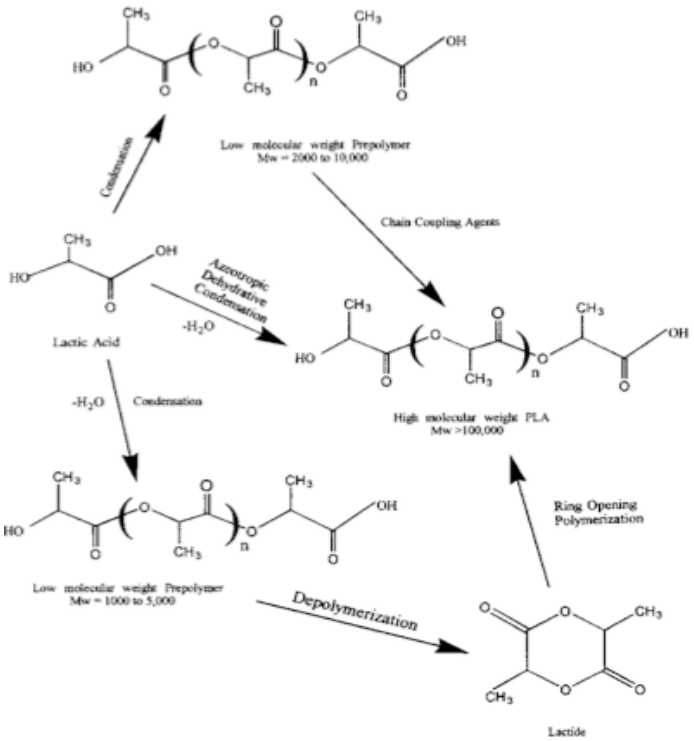

Figure 2. Syntehsis method for high molecular weight poly(lactic acid)

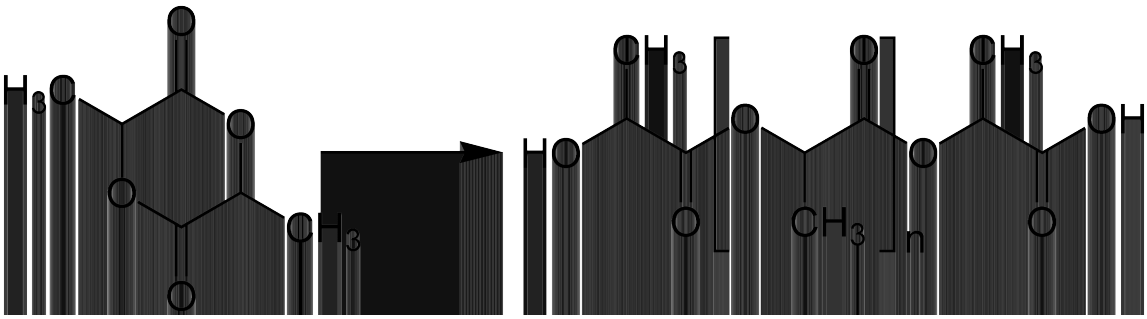

Figure 3. Synthesis of poly(lactic acid) from lactide

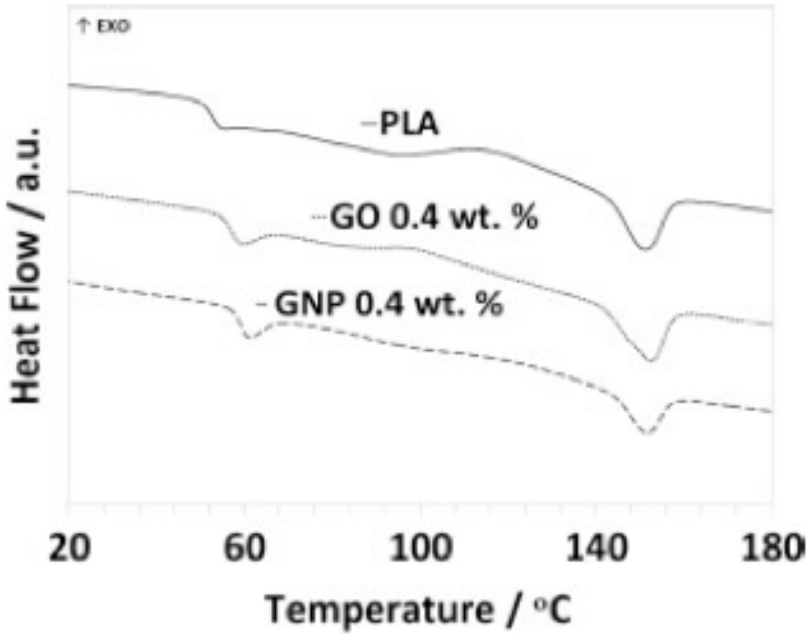

Figure 4. Differential scanning calorimetry graph of poly(lactic acid) and nanocomposites

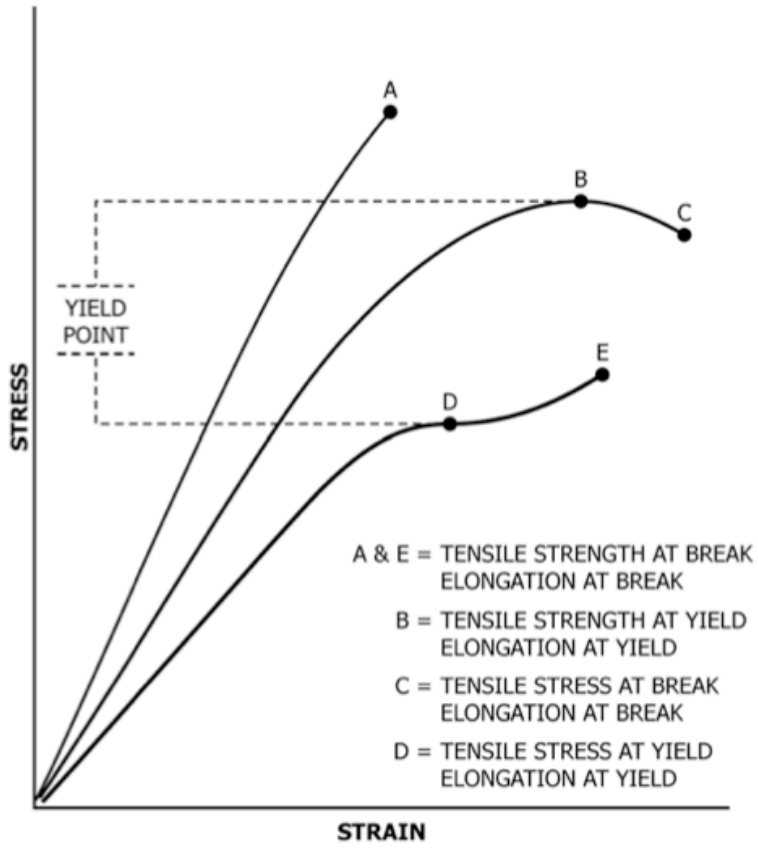

Figure 5. stress vs strain curve

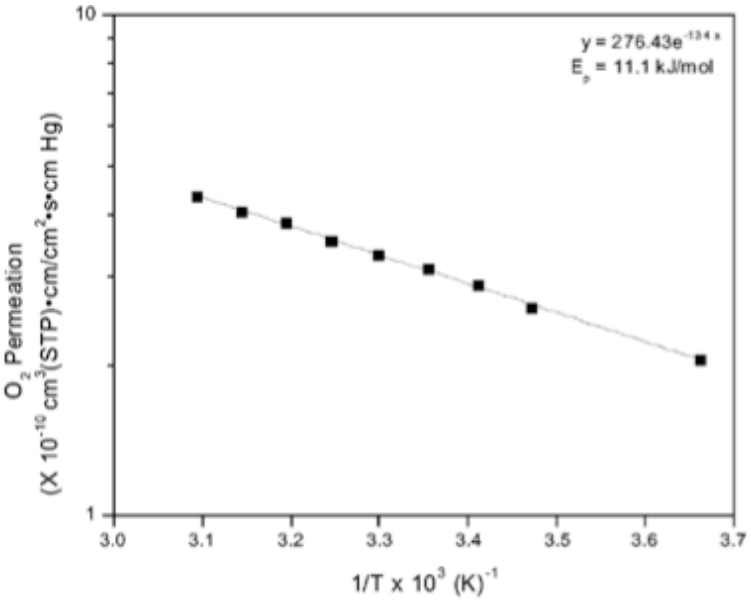

Figure 6. Temperature dependence of O_2 permeation for L:D = 96:04

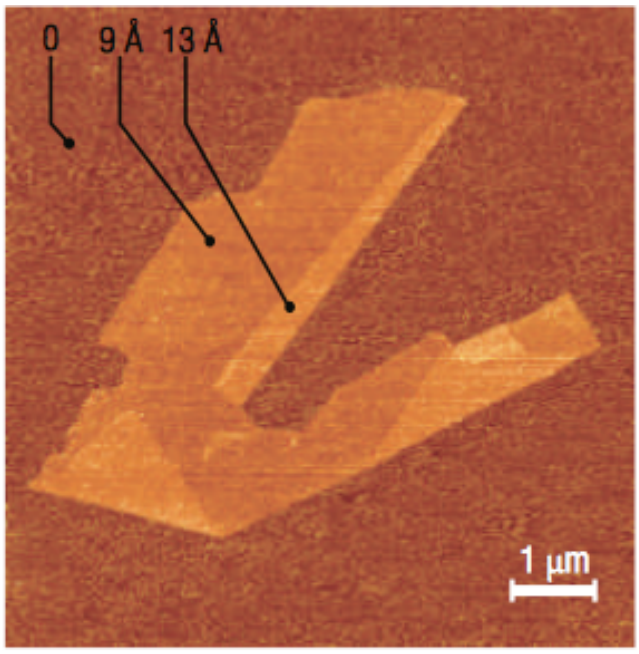

Figure 7. Graphene visualized by atomic force microscopy.

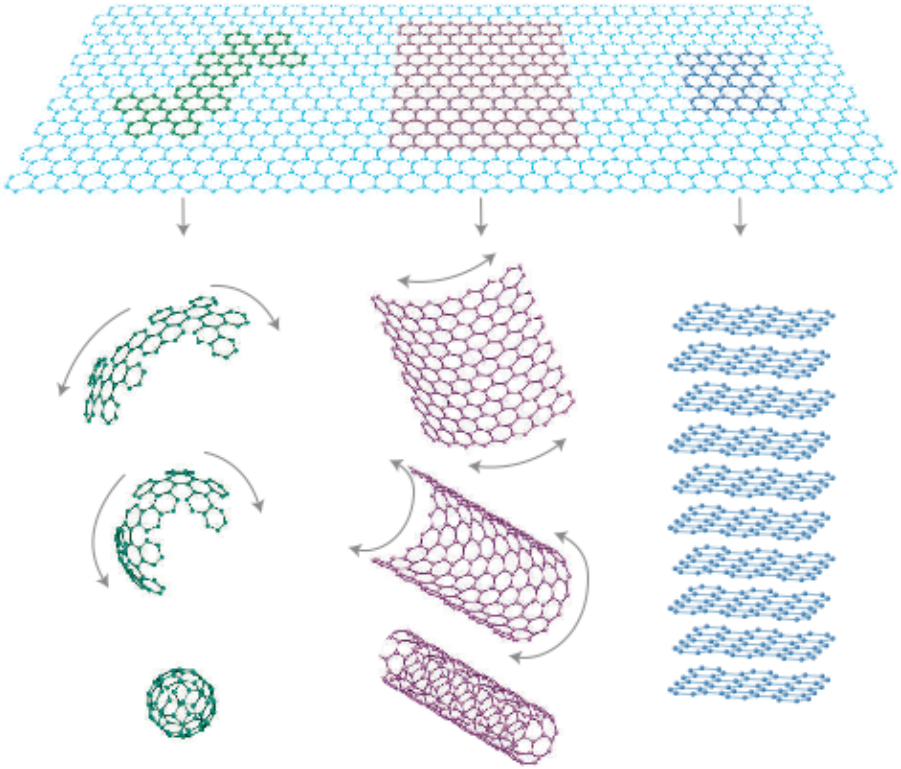
Figure 8. Graphene can form in 0, 1, 2 and 3-dimensional crystallite.

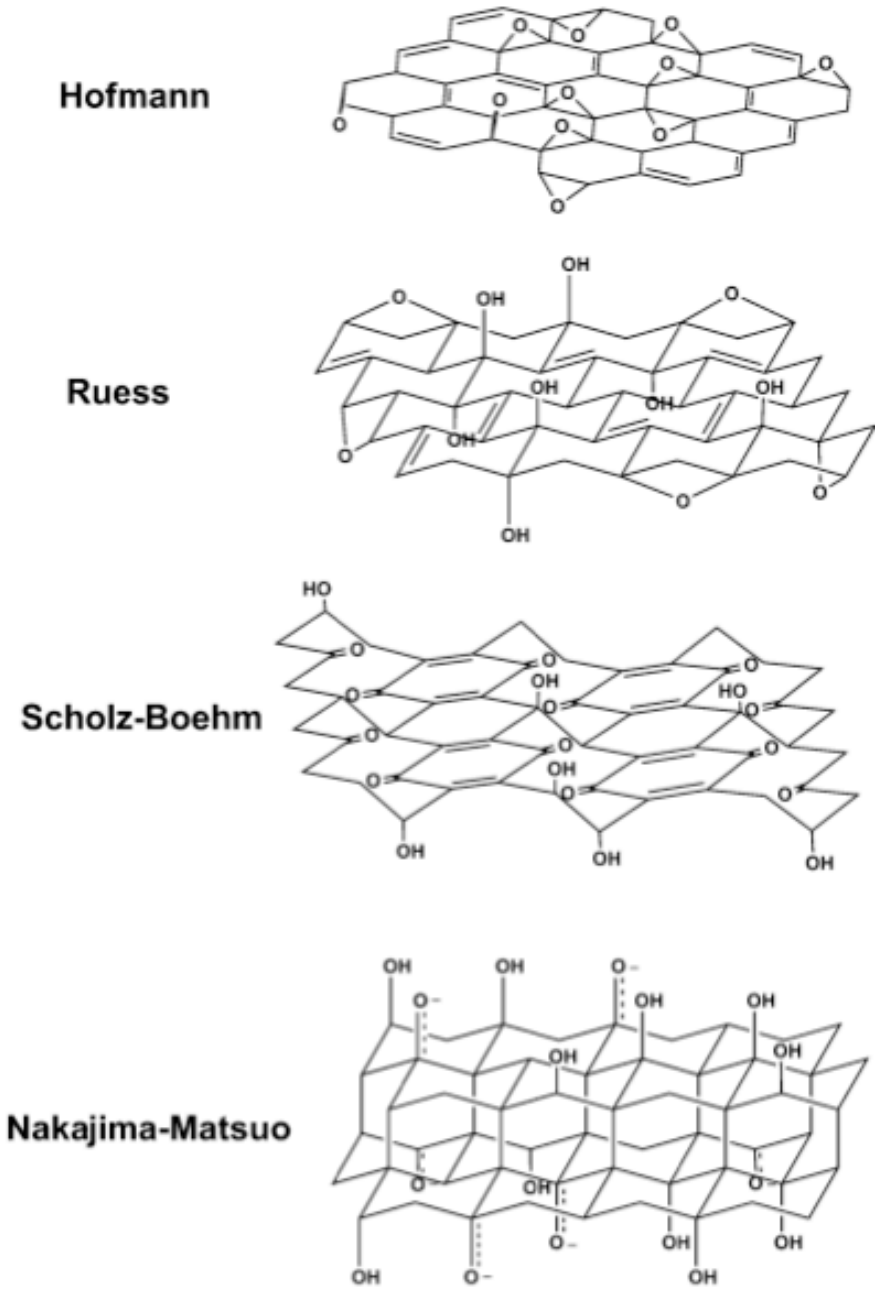

Figure 9. Summary of several older structural models of graphene oxide.

Table 1 Comparison of typical biodegradable polymer properties with LDPE, PS, and PET adapted from Clarinval and Halleux (2205).

	T_g (°C)	Tm (°C)	Tensile strength (MPa)	Tensile modulus (Mpa)	Elongation at break (%)
LDPE	−100	98 to 115	8 to 20	300 to 500	100 to 1000
PCL	−60	59 to 64	4 to 28	390 to 470	700 to 1000
Starch	–	110 to 115	35 to 80	600 to 850	580 to 820
PBAT	−30	110 to 115	34 to 40	–	500 to 800
PTMAT	−30	108 to 110	22	100	700
PS	70 to 115	100	34 to 50	2300 to 3300	1.2 to 2.5
Cellulose	–	–	55 to 120	3000 to 5000	18 to 55
PLA	40 to 70	130 to 180	48 to 53	3500	30 to 240
PHB	0	140 to 180	25 to 40	3500	5 to 8
PHA	−30 to 10	70 to 170	18 to 24	700 to 1800	3 to 25
PHB-PHV	0 to 30	100 to 190	25 to 30	600 to 1000	7 to 15
PVA	58 to 85	180 to 230	28 to 46	380 to 530	–
Cellulose acetate	–	115	10	460	13 to 15
PET	73 to 80	245 to 265	48 to 72	200 to 4100	30 to 300
PGA	35 to 40	225 to 230	890	7000 to 8400	30
PEA	−20	125 to 190	25	180 to 220	400

Table 2 Comparison of physical properties of high moleculare weight poly(lactic acid).

	Unoriented	Oriented[a]
Ultimate tensile strength(psi × 10^3, MPa)	6.9–7.7, 47.6–53.1	6.9–24, 47.6–166
Tensile yield strength (psi × 10^3, MPa)	6.6–8.9, 45.5–61.4	N/A
Tensile modulus (psi × 10^3, MPa)	500–580, 3447–4000	564–600, 3889–4137
Notched izod impact (ft-lb/in.)	0.3–0.4	N/A
Elongation at break (%)	3.1–5.8	15–160
Rockwell hardness	82–88	82–88
Specific gravity (g/cm^3)	1.25	1.25
Glass transition temperature (°C)	57–60	57–60

Table 3 Poly(lactic acid) permeability parameters.

		L:D, 96:4 (30 °C) (Lehermeier and others 2001)	L:D, 98.7:1.3 (30 °C) (Bao and others 2006)
CO_2	10^{-10} cm^3 cm/ cm^2scm Hg	1.2	1.1
O_2		3.3	0.26
N_2		1.3	0.05

Table 4 Processing possibilities of typical commercial biodegradable plymers (Clarinval 2002; Clarinval and Halleux 2005, NatureWork datasheets).

	Injection molding	Extru-sion	Extrusion blow molding	Cast film extrusion	Blow mold-ing	Fiber spinn-ing	Thermo-forming
Starch	×	×	×	×			
Cellulose	×	×			×		
PHB	×	×	×	×	×		×
PHB-PHV	×	×	×	×	×	×	×
PLA	×	×		×	×	×	×
PBS	×	×					
PCL	×	×	×		×	×	×
PBST	×	×		×			×
PBAT		×	×	×			
PTMAT		×	×	×		×	
PVA	×	×		×		×	×
PP,PE + additives	×	×	×	×	×	×	×
Starch + PVA	×	×		×	×	×	
Starch + cellulose acetate	×	×	×		×		×

Table 5 Main application of poly(lactic acid) in 2003 and the estimation for 2020 (Wolf 2005)

	Injection molding	Extru-sion	Extrusion blow molding	Cast film extrusion	Blow mold-ing	Fiber spinn-ing	Thermo-forming
Starch	×	×	×	×			
Cellulose	×	×			×		
PHB	×	×	×	×	×		×
PHB-PHV	×	×	×	×	×	×	×
PLA	×	×		×	×	×	×
PBS	×	×					
PCL	×	×	×		×	×	×
PBST	×	×		×			×
PBAT		×	×	×			
PTMAT		×	×	×		×	
PVA	×	×		×		×	×
PP,PE + additives	×	×	×	×	×	×	×
Starch + PVA	×	×		×	×	×	
Starch + cellulose acetate	×	×	×		×		×

References

Ajioka, M., et al. (1995). "BASIC PROPERTIES OF POLYLACTIC ACID PRODUCED BY THE DIRECT CONDENSATION POLYMERIZATION OF LACTIC-ACID." Bulletin of the Chemical Society of Japan 68(8): 2125-2131.

Allen, M. J., et al. (2008). "Temperature dependent Raman spectroscopy of chemically derived graphene." Applied Physics Letters 93(19).

Allen, M. J., et al. (2010). "Honeycomb Carbon: A Review of Graphene." Chemical Reviews 110(1): 132-145.

B.K., A. (1991). X-ray Spectroscopy. Berlin, Springer-verlag.

Bao, L., et al. (2006). "Gas permeation properties of poly(lactic acid) revisited." Journal of Membrane Science 285(1-2): 166-172.

Braunecker, W. A. and K. Matyjaszewski (2007). "Controlled/living radical polymerization: Features, developments, and perspectives." Progress in Polymer Science 32(1): 93-146.

Buchholz, B. (1994). 302, 694.

Cao, Y., et al. (2010). "Preparation of organically dispersible graphene nanosheet powders through a lyophilization method and their poly(lactic acid) composites." Carbon 48(13): 3834-3839.

Carrasco, F., et al. (2006). "Thermal stability of polyhydroxyalkanoates." Journal of Applied Polymer Science 100(3): 2111-2121.

Carrasco, F., et al. (2010). "Processing of poly(lactic acid): Characterization of chemical structure, thermal stability and mechanical properties." Polymer Degradation and Stability 95(2): 116-125.

Chen, D., et al. (2010). "In Situ Thermal Preparation of Polyimide Nanocomposite Films Containing Functionalized Graphene Sheets." Acs Applied Materials & Interfaces 2(12): 3702-3708.

Chollet, E., et al. (2009). "Monitoring nisin desorption from a multi-layer polyethylene-based film coated with nisin loaded HPMC film and diffusion in agarose gel by an immunoassay (ELISA) method and a numerical modeling." Innovative Food Science & Emerging Technologies 10(2): 208-214.

Datta, R. and M. Henry (2006). "Lactic acid: recent advances in products, processes and technologies — a review." Journal of Chemical Technology & Biotechnology 81(7): 1119-1129.

Doi, Y., et al. (1990). "BIODEGRADATION OF MICROBIAL COPOLYESTERS - POLY(3-HYDROXYBUTYRATE-CO-3-HYDROXYVALERATE) AND POLY(3-HYDROXYBUTYRATE-CO-4-HYDROXYBUTYRATE)." Macromolecules 23(1): 26-31.

Dorgan, J. R., et al. (2000). "Thermal and rheological properties of commercial-grade poly(lactic acid)s." Journal of Polymers and the Environment 8(1): 1-9.

Dresselhaus, M. S. and G. Dresselhaus (2002). "Intercalation compounds of graphite." Advances in Physics 51(1): 1-186.

Dreyer, D. R., et al. (2010). "The chemistry of graphene oxide." Chemical Society Reviews 39(1): 228-240.

Fernandez-Merino, M. J., et al. (2010). "Vitamin C Is an Ideal Substitute for Hydrazine in the Reduction of Graphene Oxide Suspensions." Journal of Physical Chemistry C 114(14): 6426-6432.

G. B. Kharas, F. S.-R., and D. K. Severson (1994). Plastics From Microbes: pp. 93-137.

Gao, J., et al. (2010). "Environment-Friendly Method To Produce Graphene That Employs Vitamin C and Amino Acid." Chemistry of Materials 22(7): 2213-2218.

Garlotta, D. (2001). "A literature review of poly(lactic acid)." Journal of Polymers and the Environment 9(2): 63-84.

Geim, A. K. and K. S. Novoselov (2007). "The rise of graphene." Nature Materials 6(3): 183-191.

Giles FH, W. J., Mount EM (2005). Extrusion, the definitive processing guide and handbook.

Goenka, S., et al. (2014). "Graphene-based nanomaterials for drug delivery and tissue engineering." Journal of Controlled Release 173: 75-88.

Guo, H., et al. (2013). "Preparation of reduced graphene oxide by infrared irradiation induced photothermal reduction." Nanoscale 5(19): 9040-9048.

Gupta, A., et al. (2006). "Raman scattering from high-frequency phonons in supported n-graphene layer films." Nano Letters 6(12): 2667-2673.

Hartmann, M. H. (1998). Biopolymers from Renewable Resources Springer-Verlag, Berlin.

Hassan, M., et al. (2013). "High-yield aqueous phase exfoliation of graphene for facile nanocomposite synthesis via emulsion polymerization." Journal of Colloid and Interface Science 410: 43-51.

Hassouna, F., et al. (2011). "Development of new approach based on Raman spectroscopy to study the dispersion of expanded graphite in poly(lactide)." Polymer Degradation and Stability 96(12): 2040-2047.

Hofmann, U. and R. Holst (1939). "The acidic nature and the methylation of graphitoxide." Berichte Der Deutschen Chemischen Gesellschaft 72: 754-771.

Hummers, W. S. and R. E. Offeman (1958). "PREPARATION OF GRAPHITIC OXIDE." Journal of the American Chemical Society 80(6): 1339-1339.

Inata, H. and S. Matsumura (1985). "CHAIN EXTENDERS FOR POLYESTERS .1. ADDITION-TYPE CHAIN EXTENDERS REACTIVE WITH CARBOXYL END GROUPS OF POLYESTERS." Journal of Applied Polymer Science 30(8): 3325-3337.

J. K. Lalla, N. N. C. (1990). Indian Drugs 27(10), 516-522.

Jamshidian, M., et al. (2010). "Poly-Lactic Acid: Production, Applications, Nanocomposites, and Release Studies." Comprehensive Reviews in Food Science and Food Safety 9(5): 552-571.

Jin, J., et al. (2013). "Identifying the Active Site in Nitrogen-Doped Graphene for the VO2+/VO2+ Redox Reaction." ACS Nano 7(6): 4764-4773.

Jin, T., et al. (2009). "Antimicrobial activity of nisin incorporated in pectin and polylactic acid composite films against Listeria monocytogenes." International Journal of Food Science and Technology 44(2): 322-329.

Kawai, T., et al. (2007). "Crystallization and melting behavior of poly (L-lactic acid)." Macromolecules 40(26): 9463-9469.

Kim, I.-H. and Y. G. Jeong (2010). "Polylactide/Exfoliated Graphite Nanocomposites with Enhanced Thermal Stability, Mechanical Modulus, and Electrical Conductivity." Journal of Polymer Science Part B-Polymer Physics 48(8): 850-858.

Kopinke, F. D., et al. (1996). "Thermal decomposition of biodegradable polyesters .2. Poly(lactic acid)." Polymer Degradation and Stability 53(3): 329-342.

Kricheldorf, H. R. and A. Serra (1985). "POLYLACTONES .6. INFLUENCE OF VARIOUS METAL-SALTS ON THE OPTICAL PURITY OF POLY(L-LACTIDE)." Polymer Bulletin 14(6): 497-502.

Land, T. A., et al. (1992). "STM INVESTIGATION OF SINGLE LAYER GRAPHITE STRUCTURES PRODUCED ON PT(111) BY HYDROCARBON DECOMPOSITION." Surface Science 264(3): 261-270.

Lehermeier, H. J., et al. (2001). "Gas permeation properties of poly(lactic acid)." Journal of Membrane Science 190(2): 243-251.

Lei, L., et al. (2012). "Preparing conductive poly(lactic acid) (PLA) with poly(methyl methacrylate) (PMMA) functionalized graphene (PFG) by admicellar polymerization." Chemical Engineering Journal 209: 20-27.

Lerf, A., et al. (1998). "Structure of graphite oxide revisited." Journal of Physical Chemistry B 102(23): 4477-4482.

Li, J. L., et al. (2006). "Oxygen-driven unzipping of graphitic materials." Physical Review Letters 96(17).

Loh, K. P., et al. (2010). "Graphene oxide as a chemically tunable platform for optical applications." Nature Chemistry 2(12): 1015-1024.

Lopez-Rubio, A., et al. (2004). "Overview of active polymer-based packaging technologies for food applications." Food Reviews International 20(4): 357-387.

Lunt, J. (1998). "Large-scale production, properties and commercial applications of polylactic acid polymers." Polymer Degradation and Stability 59(1-3): 145-152.

Lv, R. T., et al. (2014). "Building Complex Hybrid Carbon Architectures by Covalent Interconnections: Graphene-Nanotube Hybrids and More." ACS Nano 8(5): 4061-4069.

M. Murariu, A. L. D., L. Bonnaud, Y. Paint, A. Gallos, G. Fontaine, S. Bourbigot and P. Dubois, (2010). "Polym. Degrad. Stab." 95: 889-900.

Mehta R, K. V., Bhunia H, Upadhyay SN (2005). "Synthesis of poly(lactic acid): a reveiw." J Macromol Sci Polym Rev 45:325-49.

Mermin, N. D. (1968). "CRYSTALLINE ORDER IN 2 DIMENSIONS." Physical Review 176(1): 250-&.

Norazlina, H. and Y. Kamal (2015). "Graphene modifications in polylactic acid nanocomposites: a review." Polymer Bulletin 72(4): 931-961.

Novoselov, K. S., et al. (2012). "A roadmap for graphene." Nature 490(7419): 192-200.

Novoselov, K. S., et al. (2005). "Two-dimensional gas of massless Dirac fermions in graphene." Nature 438(7065): 197-200.

Novoselov, K. S., et al. (2005). "Two-dimensional atomic crystals." Proceedings of the National Academy of Sciences of the United States of America 102(30): 10451-10453.

Partoens, B. and F. M. Peeters (2006). "From graphene to graphite: Electronic structure around the K point." Physical Review B 74(7).

Pei, S. and H.-M. Cheng (2012). "The reduction of graphene oxide." Carbon 50(9): 3210-3228.

Peierls, R. E. (1935). "Quelques proprietes typiques des corpses solides." Ann. I. H. Poincare 5, 177-222.

Pinto, A. M., et al. (2013). "Effect of incorporation of graphene oxide and graphene nanoplatelets on mechanical and gas permeability properties of poly(lactic acid) films." Polymer International 62(1): 33-40.

Pocas, M. F., et al. (2008). "A Critical Survey of Predictive Mathematical Models for Migration from Packaging." Critical Reviews in Food Science and Nutrition 48(10): 913-928.

Pu, N.-W., et al. (2009). "Production of few-layer graphene by supercritical CO2 exfoliation of graphite." Materials Letters 63(23): 1987-1989.

Reed, S. J. B. (1993). Electron Microprobe Analysis. C. U. Press. Cambridge.

Roy, N., et al. (2012). "Modifications of carbon for polymer composites and nanocomposites." Progress in Polymer Science 37(6): 781-819.

Ruess, G. (1946). "Uber das Graphitoxyhydroxyd (Graphitoxyd)." Monatshefte Chem 76: 381-417.

Russ, J. C. (1984). Fundamentals of Energy Dispersive X-ray Analysis. London, Butterworths.

Scholz, W. and H. P. Boehm (1969). "GRAPHITE OXIDE .6. STRUCTURE OF GRAPHITE OXIDE." Zeitschrift Fur Anorganische Und Allgemeine Chemie 369(3-6): 327-&.

Schrand, A. (2005). "Polymer Sample Preparation for Electron Microscopy." Microscopy and Microanalysis 11(SupplementS02): 702-703.

Segal, M. (2009). "Selling graphene by the ton." Nature Nanotechnology 4(10): 611-613.

Shen, H., et al. (2012). "Biomedical Applications of Graphene." Theranostics 2(3): 283-294.

Shogren, R. (1997). "Water vapor permeability of biodegradable polymers." Journal of Environmental Polymer Degradation 5(2): 91-95.

Singha, A. S. and V. K. Thakur (2012). BIOPOLYMERS FROM RENEWABLE RESOURCES: AN INTRODUCTION.

Siracusa, V., et al. (2008). "Biodegradable polymers for food packaging: a review." Trends in Food Science & Technology 19(12): 634-643.

Spinu, M., et al. (1996). "Material design in poly(lactic acid) systems: Block copolymers, star homo- and copolymers, and stereocomplexes." Journal of Macromolecular Science-Pure and Applied Chemistry A33(10): 1497-1530.

Suk, J. W., et al. (2010). "Mechanical Properties of Mono layer Graphene Oxide." ACS Nano 4(11): 6557-6564.

Terrones, M., et al. (2010). "Graphene and graphite nanoribbons: Morphology, properties, synthesis, defects and applications." Nano Today 5(4): 351-372.

Tsuji, H., et al. (2006). "Water vapor permeability of poly(lactide)s: Effects of molecular characteristics and crystallinity." Journal of Applied Polymer Science 99(5): 2245-2252.

Valapa, R. B., et al. (2015). "Fabrication and Characterization of Sucrose Palmitate Reinforced Poly(lactic acid) Bionanocomposite Films." Journal of Applied Polymer Science 132(3).

Vanderweij, F. W. (1980). "THE ACTION OF TIN-COMPOUNDS IN CONDENSATION-TYPE RTV SILICONE RUBBERS." Makromolekulare Chemie-Macromolecular Chemistry and Physics 181(12): 2541-2548.

Wachsen, O., et al. (1997). "Thermal degradation of poly-L-lactide - Studies on kinetics, modelling and melt stabilisation." Polymer Degradation and Stability 57(1): 87-94.

Wang, H. and Z. Qiu (2011). "Crystallization behaviors of biodegradable poly(L-lactic acid)/graphene oxide nanocomposites from the amorphous state." Thermochimica Acta 526(1-2): 229-236.

Williams, G. and P. V. Kamat (2009). "Graphene-Semiconductor Nanocomposites: Excited-State Interactions between ZnO Nanoparticles and Graphene Oxide." Langmuir 25(24): 13869-13873.

Xu, J.-Z., et al. (2010). "Isothermal Crystallization of Poly(L-lactide) Induced by Graphene Nanosheets and Carbon Nanotubes: A Comparative Study." Macromolecules 43(11): 5000-5008.

Yang, J.-H., et al. (2012). "Preparation and characterization of poly(L-lactide)-graphene composites using the in situ ring-opening polymerization of PLLA with graphene as the initiator." Journal of Materials Chemistry 22(21): 10805-10815.

Yoon, O. J., et al. (2011). "Nanocomposite nanofibers of poly(D, L-lactic-co-glycolic acid) and graphene oxide nanosheets." Composites Part a-Applied Science and Manufacturing 42(12): 1978-1984.

Yoshimura, N. (2014). Introduction of the Electron Microscope. Historical Evolution toward Achieving Ultrahigh Vacuum in Jeol Electron Microscopes: 1-10.

CHAPTER 3: IMPROVED PROPERTIES OF POLY(LACTIC ACID) WITH INCORPORATION OF CARBON HYBRID NANOSTRUCTURE

Abstract

In the current work, the incorporation of nanocomposite of graphene oxide (GO) and single-walled carbon nanotube (SWCNT) into poly(lactic acid) is investigated in detail. The influence of GOCNT nanocomposite in aspect of crystalline, thermal, oxygen barrier, mechanical, optical and morphological properties has been studied. Field emission scanning electron microscope observes minor coagulation of GOCNT nanocomposite. X-ray diffraction determines influence of GOCNT nanocomposite on crystallinity of poly(lactic acid). Differential scanning calorimetry confirms no significant shift of glass transition temperature and melting temperature due to GOCNT nanocomposite. The significant improvement of ultimate tensile strength and oxygen transmission rate are observed in this work.

Introduction

Over the past decades, research interest on biopolymer films has been drastically increased. Due to depletion of petroleum resources, biopolymer becomes a promising substitute material of polymer product. Biopolymer derived from renewable resources giving superior biodegradability which has great impact on environment in long term.

Poly(lactic acid) is one of the most potential representative biopolymer which recently has become familiar in packaging industry. Poly(lactic acid) is considered as biodegradable and biocompatible polymer. Poly(lactic acid) is aliphatic polyesters derived from alpha-hydroxy acids. It can be modified by polymerization of the mixture L and D isomers which determine the molecular weight and crystalline of structure (Norazlina and Kamal 2015). While poly(lactic acid) has great advantages, it is challenge to be massive industrialized due to poor properties such as mechanical, gas barrier and thermal (Barlow and Morgan 2013). Since it is necessary to tailor poly(lactic acid) to substitute packaging materials, incorporation of nanofillers has been introduced. Incorporation of nanofillers and improvement of targeted property have been reported within various research such as graphene oxide, citrate esters, and clays (Alboofetileh, Rezaei et al. 2013). Poly(lactic acid) composite with graphene based material presents

evidence of potential improvement on mechanical, thermal and gas barrier properties (Norazlina and Kamal 2015).

Graphene oxide (GO) has been introduced recently as a potential nanofiller for biopolymer production. It has number of outstanding properties including heat conductivity, mechanical strength, and resistance to chemicals (Hu, Kulkarni et al. 2014). GO is still a two-dimensional sheet configuration as graphene. GO has less portion of π-electronic network compared to graphene due to oxidation (Norazlina and Kamal 2015). Exfoliated GO tends to have less aggregation behavior than graphene and graphite. However, strong van der Waals interaction still causes irreversible agglomerates and poor dispersion on organic matrix (Du and Cheng 2012). Here single-walled carbon nanotube (SWCNT) is introduced to GO. SWCNT prevents van der waals interaction of GO causing less coagulation and even dispersion on poly(lactic acid) (Raquez, Habibi et al. 2013). GOCNT nanocompoiste is prepared by solution blending which is beneficial on nanomaterials dispersion in polymer matrix than in situ polymerization blending and melt blending (Roy, Sengupta et al. 2012). In this work, composite of GO and SWCNT (GOCNT nanocomposite) is incorporated into poly(lactic acid) with different weight percentage loading. In aspect of thermal, mechanical and gas barrier property, influence of GOCNT nanocomposite has been studied.

Materials and Methods

Materials

Poly(lactic acid) was obtained from NatureWorks LLC (7000D) with a D content of 4.25 wt%, a residual monomer content of 0.3 wt%, melt density 1.08g/cm^3, molecular weight 113,000g/mol, glass transition temperature and a melting pint of 60 and 155^{o}C respectively. Poly(lactic acid) was completely dried in vacuum oven with 40^{o}C before each use. Graphite (powder, <20micron meter, molecular weight 12.01 g/mol) and single-walled carbon nanotube (SWCNT, diameter 0.7 nm and density 1.7 g/cm^3) were obtained from Sigma Aldrich, USA.

Preparation of exfoliated graphene oxide

Exfoliated graphene oxide was synthesized and followed by Hummers' method with minor modification ((Hummers and Offeman 1958). 10g of graphite was added to 250mL of H_2SO_4 at the room

temperature. The solution was cooled in ice bath under 5^{o}C followed by gradual addition of 35g $KMnO_4$. The solution was heated to 35^{o}C for 12 hours. The solution was cooled again in ice bath. Excess H_2O_2 was gradually added to reduce unreacted $KMnO_4$ until bubbles and bright yellow presented. Distilled water was repeatedly added to solution until the solution reached to pH 7. Precipitate of solution was secured and remain solution was removed repeatedly to obtain pH 7. Secured mud-like graphene oxide was transferred to falcon tube and centrifuged to increase precipitation yield of graphene oxide with small amount of solution. Using liquid nitrogen immediately froze neutralized graphene oxide. Exfoliated graphene oxide was obtained as powder using freezing drier of neutralized solution. Obtained powder of graphene oxide was stored in vacuum desiccator.

Preparation of PLA-GOCNT nanocomposite

PLA-GOCNT nanocomposite films were prepared by a simple solution casting method following by GOCNT nanocomposite preparation. GOCNT nanocomposite was followed by the method of Tian et al, with minor modification (Tian, Meziani et al. 2010). Graphene oxide and SWCNT in 3 to 1 mass ratio respectively added to 180mL of chloroform separately. The mixture was ultra-sonicated until homogeneous dispersion was observed visually (Solution 2) (Sun, Wang et al. 2014). The mass ratio of graphene oxide and SWCNT was determined following by Sun et al. At the ratio of 3:1, the nanomaterials performed greatest specific capacity and specific surface area (Sun, Wang et al. 2014).

10g of Poly(lactic acid) was dissolved in 100mL of chloroform for 2 hours (Solution 1) with magnetic stirring bar. Solution 2 was dispersed in solution 1 gradually to avoid aggregation of nanocomposite (Solution 3) while magnetic stirring bar presented. The solution 3 underwent sonic bath for 15 minute and vacuum until bubble were not observed. Finally the solution 3 was casted on polytetrafluoroethylene-coated plate and air dried for 1 week. Once PLA-GOCNT nanocomposite films were dried, they were removed from coated plate and placed in zip lock bag. Films were dried again for another week in vacuum oven at 40^{o}C. Films were stored in vacuum oven until use. The overall preparation is described in Fig. 2. Neat poly(lactic acid) film (PLA film) and PLA-GOCNT nanocomposite films with 0.05, 0.2, 0.3 and 0.4 wt% were prepared.

Characterization

X-ray diffraction analysis (XRD)

XRD analysis of synthesized graphene oxide, neat poly(lactic acid) films and PLA-GOCNT nanocomposite films were carried out at room temperature on the Bruker D8 XRD with radiation operating at 40 kV and 40 mA. The diffraction data were collected in the 2-theta range of 5 to 60^{o} with scanning rate of 4^{o} per minute. Base line correction was performed to have acute comparison among each XRD graphs. Percentage crystallinity (%X_c) of each films were calculated by following:

$$\%X_c = \frac{\text{Total area of crystalline peaks}}{\text{Total area of all peaks}} \text{ x } 100\% \quad (1)$$

Morphological analysis

The morphology of GOCNT nanocomposite dispersion among poly(lactic acid) film was imaged by Field emission scanning electron microscope (LEO Zeiss 1550) operated at 2.00 kV. PLA-GOCNT nanocomposite films were sampled on aluminum pin disc coated with iridium for 2nm thickness.

Differential scanning calorimetry (DSC)

Crystallization and thermal behavior of neat poly(lactic acid) film and PLA-GOCNT nanocomposite films were studied using a differential scanning calorimeter (Discovery DSC). Films (5 ± 0.5mg) are scaled and secured in aluminum pans. Films were heated from 20^{o}C at a heating rate of 5^{o}C min^{-1} in the N_2 atmosphere. Thermal history of the films was eliminated during first heating cycle. Films were cooled with rate of -5^{o}C min^{-1}. Glass transition temperature (T_g), melting temperature (T_m), enthalpy change at T_c (ΔH_c), enthalpy of fusion at T_m (ΔH_m), and percentage crystallinity (%X_c) for neat poly(lactic acid) films and PLA-GOCNT nanocomposite films were reported through DSC thermograph from second heating cycle. Following

$$\%X_c = \frac{(\Delta H_m - \Delta H_c)}{(\Delta H_{mp})} \times 100\% \quad (2)$$

equation was adopted to calculate percentage crystallinity where ΔH_{mp} is the enthalpy of 100 percent crystalline (for PLA = 93.6 Jg^{-1}) (Valapa, Pugazhenthi et al. 2015).

UV-visible spectrophotometer analysis

UV-visible spectrometer (Lambda 25 Spectrophotometers) was adopted to test transparency of films. Films, stored in vacuum oven, were used. The range of wavelength was 190-790 nm with a scanning rate 50nm min^{-1}.

Mechanical test

Ultimate tensile strength (UTS) and tensile modulus were measured on room temperature condition using ADMET with a 200 N load cell and 5 mm min^{-1} fixed test speed. Films were prepared as described as ASTM D882 (Gauge length of 30mm and gauge width of 20mm). Five specimens for each film were measured and average thickness of films were measured as 60 ± 5 micron. Films were stored in humidity control chamber (55% humidity and room temperature) for 48 hours before being tested.

Oxygen transmission rate (OTR)

Oxygen barrier property was studied by measuring oxygen transmission rate at room temperature in 1atm (OxySense 5250I). Film dimension was around 3 inch by 3 inch and thickness was measured. Prepared film was placed inside chamber using adhesive vacuum grease. 99.99% pure O_2 and N_2 were purged into driving well and sensing well respectively. O_2 and N_2 were purged for 1 minute and 4 minutes respectively with flowing rate under 1mL/min. Data of five specimens were collected for each type of film and at least 10 oxygen readings were collected in every 5 minutes for each film. Oxygen transmission rate was read once oxygen concentration graph reached to steady line (horizontal to x-axis). The average thickness was measured (60 ± 5 micron) before OTR test.

Result and Discussion

XRD analysis of GOCNT nanocomposite

The XRD pattern of GOCNT nanocomposite is shown in Fig. 3a. The spectrum of GOCNT nanocomposite exhibits a strong (001) diffraction peak at $\theta = 12.25^{o}$ corresponding to 0.75nm of interlayer spacing. This interlayer spacing indicates the existence of intercalation of oxygen functional groups (Lee and Park 2014). At $\theta = 25.68^{o}$, weak and broad peak (002) is found which is derived from graphite-like structure of SWCNT. This also indicates that stacked graphene single layers with distance of 0.335 nm are found, but small amount due to extremely low intensity of peak compared to peak at $\theta = 12.25^{o}$ (Murariu, Dechief et al. 2010). Compared to Fig. 3b graphene oxide with multi-walled carbon nanotube (GO/aMWCNT), GOCNT nanocomposite shows similar pattern (Sun, Wang et al. 2014).

XRD analysis of neat poly(lactic acid) and PLA-GOCNT nanocomposite film

Neat Poly(lactic acid) film and and PLA-GOCNT nanocomposite film structures were analyzed by X-ray diffraction (XRD) to study crystalline. On Fig. 4, no major peaks are found near 26.5^{o} for GOCNT nanocomposite loaded films. Aggregation of graphene oxide in Poly(lactic acid) film is commonly reported (M. Murariu 2010). Absence of peak at 26.5^{o} suggests that the dispersion of GOCNT nanocomposite in Poly(lactic acid) is close to a single sheet level and no restacked GO are found (Valapa, Pugazhenthi et al. 2015). It can be assumed that non-polar SWCNT aided dispersion of GO in poly(lactic acid) matrix. This can be compared to work of Wu et al in Fig. 4c. Simple graphene oxide and poly(lactic acid) were composited and demonstrated sharp peak with considerably high intensity at 25.68^{o}. This indicates the typical aggregation of graphene oxide within poly(lactic acid) matrix (Wu, Cheng et al. 2013). In Fig. 4b each film shows either sharp or broad peak (110) at 16.7^{o} and small peak at 18.5^{o} (203). These peaks represent the crystal structure of poly(lactic acid) (Valapa, Pugazhenthi et al. 2015). Percentage crystallinity ($\%X_c$) was calculated followed by equation (1) and shown on Table 1. Percentage crystallinity increases as GOCNT nanocomposite weight percentage increases, but cannot be considered as significant. Therefore, GOCNT nanocomposite did not significantly modify crystal structure of poly(lactic acid) in the nanocomposite. This result can be compared with XRD data from group of Wang as shown in Fig. 4b (Wang and Qiu 2011). Group of Wang studied on effect of GO incorporation on poly(L-lactic acid)

(PLLA) in the aspect of crystallinity. Fig. 4b has two sharp peaks at 16.3^{o} (110)/(200) and 18.7^{o} (203) for both neat PLLA and GO incorporated PLLA. Group of Wang concluded that crystal structure of PLLA has not been changed with present of GO. This crystallinity data will be further compared and discussed more in DSC data.

Morphological analysis

FE-SEM has been conducted to observe dispersion of GOCNT nanocomposite on poly(lactic acid) matrix. FE-SEM image is valuable feature to determine the dispersion and interfacial bonding of GOCNT nanocomposite and poly(lactic acid) (Fu, Liu et al. 2014). Image shown in Fig. 5 demonstrates homogeneous dispersion of GOCNT nanocomposite. White portions (red arrow) are GOCNT nanocomposite that barely found in neat PLA and PLA-GOCNT-0.05. White portions are increased as wt% of GOCNT nanocomposite increases. Selected portion (yellow mark) is magnified to observe coagulation of GOCNT nanocomposite. Even though Fig. 5f has highest wt% of GOCNT nanocomposite, great dispersion behavior is observed in poly(lactic acid) matrix.

GO is well known to have well-dispersed aqueous colloids in both organic and inorganic sovlents (Bourlinos, Gournis et al. 2003). GO is highly negatively charged in aqueous solvent since ionization of abundant carboxylic and hydroxyl groups. Due to strong electrostatic repulsion of GO with solvents as well as its hydrophilicity, GO itself shows great dispersion in poly(lactic acid) matrix as shown in Fig. 5 (Szabo, Berkesi et al. 2006). However, even if GO great dispersion ability, agglomeration of nanocomposite is still found as Fig. 5c red arrow. GO, which was chemically reduced and ultrasonicated from graphite oxide, tends to have irreversible agglomeration itself due to strong Van der Waals forces among GO sheets (Lei, Qiu et al. 2012). To solve the agglomeration, in this work, SWCNT was incorporated to GO to build hybrid nanostructure that reduce agglomeration of the nanocomposite. SWCNT in the hybrid nanostructure prevents coagulation of GO by interfering Van der Waals forces among GO sheets (Raquez, Habibi et al. 2013). In Fig. 5, agglomerated GOCNT nanocomposite are rarely found among different weight loaded films and this result is confirmed by XRD data.

Transparency

From Fig. 6, neat PLA has 65% and 75% of transmittance at 250nm and 300nm respectively. This indicates that neat PLA allows most of UV-B light through film. UV-B region (280-315 nm) causes critical photochemical degradation of plastics (Valapa, Pugazhenthi et al. 2015). Compared to neat PLA, PLA-GOCNT-0.4 has 40% and 50% transmittance of 250nm and 300 nm respectively, which is notable improvement in UV-B light prevention. Around 85% of Visible light (575 nm) transmits through neat PLA. PLA-GOCNT-0.4 only allows 58% of visible light so that it has less transparency compared to neat PLA. Fig. 7 shows the optical transparency of each film.

Mechanical properties

Generally, the incorporation of nanofillers into polymer is expected to improve mechanical properties such as tensile strength, elasticity etc. Fig. 8 shows the ultimate tensile strength (UTS) and tensile modulus properties of neat PLA and PLA-GOCNT nanocomposite films. Higher wt% of GOCNT nanocomposite is observed to have higher ultimate tensile strength. Compared to neat PLA, the UTS of PLA-GOCNT-0.4 is 1.75 times stronger which is significant improvement. It has been reported that UTS decreases at certain wt% of nano-contents due to poor dispersion on poly(lactic acid) matrix. This is significant that Fig. 8 exhibits different trend compared to others shown in fig. 9 (Valapa, Pugazhenthi et al. 2015), (Pinto, Cabral et al. 2013) and (Buasri, Patwiwattanasiri et al. 2015). Valapa et al. obtained strongest UTS at the lowest graphene loaded. 0.4 wt% GOCNT has highest UTS, which is significant result compared to Valapa et al. It indicates the successful dispersion of high wt% GOCNT in PLA matrix. It can be assumed that hybrid nanostructure of GOCNT have greater dispersion and adhesion in poly(lactic acid) matrix than simple GO or graphene (Fang, Wang et al. 2009). One of the greatest advantages of graphene is self-lubricating behavior due to weak Van der Waals forces bonding among graphene sheets allowing interlamellar sliding (Murariu, Dechief et al. 2010). However once graphene loses the benefit within PLA matrix due to strong hydrogen bond between ester groups of PLA and oxygen-containing functional group of graphene (Fang, Wang et al. 2009). Fig. 8b shows linear relationship between tensile modulus and wt%

of GOCNT nanocomposite. PLA-GOCNT-0.2 has exceptionally high tensile modulus, which induced by the agglomeration of GOCNT nanocomposite responsible for greatest brittleness of PLA matrix.

Table 6 a and b show statistical analysis of UTS and young's modulus with Tukey method. Number of replicates were 5 per control and randomly selected. As shown in the table, each weight percent of GOCNT demonstrate significant differences among each other. P-value is less than 0.05, which also proves significant differences.

Oxygen transmission rate (OTR)

Poly(lactic acid) is semi-crystalline polymer which mostly consists of amorphous region. This amorphous region allows the permeation and diffusion of oxygen molecule. Recently, impermeable nanoplatelets are introduced to improve gas barrier property by creating tortuous pathway (Chen, Fu et al. 2014). Furthermore, gas barrier property is closely related to polymer's crystallinity and crystalline morphology (Huang, Ren et al. 2014). However, as shown in table 4, crystallinity of each film did not significantly increase. Films with different weight percent load are considered as amorphous. Therefore, OTR more depends on improving dispersion of GOCNT nanocomposite than change of crystallinity (Huang, Ren et al. 2014). Here are the three major factors affect the torturous path effect: the volume fraction of GOCNT nanocomposite; morphology of GOCNT nanocompostie such as exfoliation, dispersion etc; and their aspect ratio (Lape, Nuxoll et al. 2004). The successful dispersion of GOCNT nanocomposite was confirmed by FESEM images and XRD graph. Regardless of the morphology, the interactions between GOCNT nanocomposite and poly(lactic acid) also affect oxygen impermeability of film. The strong interfacial adhesion is due to hydrogen bonding between ester group of poly(lactic acid) and oxygen-containing functional group of GO. Furthermore few researcher groups assumed that mechanical interlocking structure of nanoplatelets and polymer causes interfacial adhesion (Huang, Ren et al. 2014). Such factors can constrain the mobility of polymer chain, reduce the free volume in the interfacial region and densify the polymer matrix (Compton, Kim et al. 2010). In this work, GOCNT nanocomposite performed as impermeable barriers to the diffusing gas molecules and lead them to longer and more tortuous pathway in poly(lactic acid) matrix. Table 2 shows that OTR decreases as GOCNT nanocomposite wt% increases. PLA-GOCNT-0.4 achieved 66.57% reduction in OTR compared to neat PLA. Table 3 is

references of oxygen barrier property by others (Valapa, Pugazhenthi et al. 2015), (Pinto, Cabral et al. 2013). Both Table 3a and 3b demonstrate decrease of gas barrier property at highest wt% content due to graphene oxide aggregation at higher loading.

Table 7 shows statistical data for oxygen transmission rate with 5 different replicates per control in random selection. P-value is less than 0.05 and each weight percent of GOCNT are significantly different among each other except neat-PLA and PLA-GOCNT-0.05.

Differential scanning calorimetry (DSC)

Fig. 10 and Table 4 display thermal behavior of neat PLA and PLA-GOCNT nanocomposite films. Endothermic peaks are found at 57 to 58 ^{o}C corresponding to the glass transition temperature. There was slight T_g shift for GOCNT nanocomposite loaded films compared to neat PLA but not a significant change. It can be assumed that GOCNT nanocomposite does not affect formation of short chain PLA molecules (L. Liu 2009). Another unimodal endothermic peaks are found at 154 ^{o}C as melting temperature. T_m has minor shift towards left but it is also considered as not a significant change. Even if it is insignificant change, GOCNT nanocomposite still can be considered as an effective nucleating agent to sustain crystallization behavior of (Valapa, Pugazhenthi et al. 2015). Wu et al. researched on graphene as a nucleating agent of polylactid crystallization (Wu, Cheng et al. 2013). Lauritzen-Hoffman-Miller theory was used to explore graphene's nucleation role during melt crystallization and cold crystallization. In this work, Wu et al. calculated the energy needed for formation of nuclei of critical size (K_g) and folding surface free energy (σ_e) for PLA and PLA-graphene nanocomposite. Both K_g and σ_e of PLA-graphene nanocomposite was reduced compared to neat PLA. This indicates that presence of nanocomposite need less energy to form nuclei of critical size and have a lower barrier for nucleation (Iannace and Nicolais 1997). Less energy is consumed by PLA chain when folded on surface of crystallizations nucleation (graphene) to form spherulites than for neat PLA (Wu, Cheng et al. 2013).

Double melting peaks are often found in nanocomposite polymer. Huang et al. studied on effect of incorporation of different volume percentage of GO on PLA. Double melting peaks are usually found only in heating rate of 10 and 20 ^{o}C/min (Huang, Ren et al. 2014). Generally, double melting peaks appear due to presence of crystals with different crystalline forms and different degree of perfections (Qiu, Xu et al.

2008). Current work shows unimodal endothermic peak of T_m explains that uniform crystal thickness and homogeneous distribution of crystals were developed during recrystallization (R. Valapa 2014).

Cold crystallization temperature (T_c) has also been observed and shown in table Table 4. As increasing weight percentage of GOCNT nanocomposite, peak temperature of T_c decreased. This indicates that non-isothermal crystallization behavior of poly(lactic acid) was improved by presence of GOCNT nanocomposite. In Figure 10, PLA-GOCNT-0.4 has largest area and lowest T_c peak temperature. This data also can be compared to % crystallinity that PLA-GOCNT-0.04 has highest crystallinity as expected. However opposite T_c trend has been reported by Wu et al. Cold crystallization temperature was increased as presence of graphene nanosheet which reduces poly(lactic acid) chain mobility and hinders crystal growth (Wu, Cheng et al. 2013). These incompatible observations are due to difference in bulk poly(lactic acid) used such as stereo structure of the poly(lactic acid) chain and D/L ratio of the poly(lactic acid). In addition to, the size and compatibility of nanofillers could be a reason. The different dispersion state of nanofillers could influence the crystallization of poly(lactic acid) (Krikorian and Pochan 2004). The relationship between Tc and heating rate in non-isothermal crystallization has been reported by Wang and Qiu. Prepared GO-PLA nanocomposites were heated in different heating rate: 5, 10, 15 and 20 ^{o}C/min. The degree of T_c change was more significant as heating rate increased (Wang and Qiu 2011). This work indicates that crystallization of poly(lactic acid) can be determined not only by nanofillers effect but also complexity of different factors.

Percentage crystallinity is shown on Table 4. There is increase of crystallinity as wt% of GOCNT nanocomposite increase. Unexpected drop of X_c is found at PLA-GOCNT-0.3 assumed due to aggregation of GOCNT nanocomposite during recrystallization. Overall, the change of crystallinity is not considered as significant. It can be assumed that the GOCNT nanocomposite does not have significant influence on crystal structure of PLA. Furthermore, due to extremely small amount of GOCNT nanocomposite was incorporated, there were insignificant crystallinity change found. This percentage crystallinity trend can be compared to XRD crystallinity table (D. Sawai 2003).

Conclusion

GOCNT nanocomposite was incorporated as a set of PLA-GOCNT nanocomposite film with different wt% loading of GOCNT nanocomposite from 0 to 0.4wt%. FESEM depicted successful dispersion of GOCNT nanocomposite on PLA matrix and barely found coagulation. XRD and DSC data shared same pattern of percentage crystallinity. As wt% load increased, $\%X_c$ increased with exception on PLA-GOCNT-0.3. The presence of GOCNT nanocomposite did not have significant effect on T_m and T_g found by DSC data. This indicates that GOCNT nanocomposite still act as nucleating agent for poly(lactic acid) crystallization process. More than 50% of UV-B light was prevented due to GOCNT nanocomposite while it reduced the transparency of film around 30% transmittance of visible light compared to neat PLA film. The ultimate tensile strength and wt% GOCNT nanocomposite have linear relationship. The maximum UTS has been found on PLA-GOCNT-0.4 which increased 67.8% of neat PLA film UTS which indicate that GOCNT nanocomposite performed good adhesion with poly(lactic acid) matrix. Oxygen barrier property also increased as load of GOCNT nanocomposite increased. Lowest oxygen transmission rate has been found at PLA-GOCNT-0.4 which reduced 66.57% of OTR compared to neat PLA film.

Supplementary

Energy Dispersive X-ray Spectrometry (EDS) has been performed to determine contamination of nanocomposite. During process of nanocomposite, ultrasonic method was applied to disperse graphene oxide and carbon nanotube in chloroform solvent. Ultrasonic rod, which is made of Titanium, was placed in the solution and titanium contamination was suspected. Figure 11. and table 5 show the identification of atoms and concentration of each atom in nanocomposite. The analysis was performed in two different region of the nanocomposite and Titanium has not been found. Sample was prepared and coated with 2nm thickness of Iridium.

Mass ratio of GO to SWCNT (3:1) was determined followed by Sun et al. The authors demonstrated the specific capacitance and specific surface area of GO/MWCNT in different mass ratio. Figure 12 shows the highest specific capacity and surface area achieved at ratio of 3:1. The authors concluded that MWCNT impeded the stacking of GO and effectively enlarged the space between GO sheets (Sun, Wang et al. 2014).

Tables

Table 1 XRD % Crystallinity

Sample name	Total area of crystalline peaks	Total area of all peaks	%crystallinity (%X_c)
PLA film	**224.7**	**452.0**	**49.71**
PLA-GOCNT-0.05	**224.6**	**451.9**	**49.70**
PLA-GOCNT-0.2	**219.4**	**429.8**	**51.05**
PLA-GOCNT-0.3	**207.4**	**412.8**	**50.24**
PLA-GOCNT-0.4	**111.9**	**196.4**	**56.98**

Table 2 Oxygen transmission rate of neat PLA and PLA-GOCNT nanocomposite films

Sample name	Temperature (^oC)	OTR (ml/m^2/day)	% Reduction in oxygen transmission rate
neat PLA	**25**	**729.09**	**n/a**
PLA-GOCNT-0.05	**25**	**739.96**	**n/a**
PLA-GOCNT-0.2	**25**	**542.80**	**25.55**
PLA-GOCNT-0.3	**25**	**324.41**	**55.50**
PLA-GOCNT-0.4	**25**	**243.72**	**66.57**

Table 3 references of oxygen barrier property (a) OTR by Valapa et al. (b) O_2 permeability by Pinto et al.

Sample name	OTR ($ml/m^2/day$)
PLA	383.33
PLA-GR-0.1	300.00
PLA-GR-0.3	333.33
PLA-GR-0.5	366.67

(a)

Sample name	O_2 Permeability ($x10^{-18}m^2s^{-1}Pa^{-1}$)
PLA	3.76
GO 0.2 wt%	1.34
GO 0.4 wt%	1.23
GO 0.6 wt%	1.49

(b)

Table 4 DSC results for neat PLA and PLA-GOCNT nanocomposite films.

Sample name	T_g (^oC)	T_m (^oC)	T_c (^oC)	ΔH_m (Jg^{-1})	ΔH_c (Jg^{-1})	X_c (%)
neat PLA	**58.4**	**154.1**	**129.3**	**2.99**	**1.71**	**1.37**
PLA-GOCNT-0.05	**57.7**	**154.0**	**129.2**	**2.40**	**1.12**	**1.36**
PLA-GOCNT-0.2	**57.5**	**153.7**	**127.2**	**5.22**	**3.08**	**2.28**
PLA-GOCNT-0.3	**57.4**	**153.5**	**126.9**	**3.44**	**1.55**	**2.02**
PLA-GOCNT-0.4	**57.4**	**153.9**	**126.9**	**5.43**	**2.97**	**2.62**

[a] **T_g = glass transition temperature, T_m = melting temperature, T_c = cold crystallization temperature, ΔH_m = enthalpy of melting, ΔH_c = enthalpy of cold crystallization, X_c = % crystallinity**

Table 5 EDS analysis composition of PLA-GOCNT nanocomposite filme (a) region 1 (b) region 2.

Element	Weight%	Atomic%
C K	52.66	61.22
O K	42.22	36.85
Si K	1.18	0.59
Cl K	3.27	1.29
Ti K	0.01	0.00
Ir M	0.66	0.05
Totals	100.00	

(a)

Spectrum 4:

Element	Weight%	Atomic%
C K	53.18	61.59
O K	42.16	36.66
Si K	1.06	0.52
Cl K	3.02	1.19
Ti K	-0.01	0.00
Ir M	0.58	0.04
Totals	100.00	

(b)

Table 6 Tukey method statistical data for (a) UTS (b) Young's moudlus

(a)

Analysis of Variance

Source	DF	Adj SS	Adj MS	F-Value	P-Value
Filler Content (wt%)_2	4	3116.40	779.099	185.90	<0.0001
Error	20	83.82	4.191		
Total	24	3200.22			

Means

Filler Content (wt%)_2	N	Mean	StDev	95% CI
0	5	40.9414	0.6490	(39.0317, 42.8511)
0.05	5	43.6922	0.8597	(41.7825, 45.6019)
0.2	5	59.682	4.132	(57.773, 61.592)
0.3	5	64.4446	0.7818	(62.5349, 66.3544)
0.4	5	68.7062	1.4511	(66.7965, 70.6159)

Pooled StDev = 2.04717

Grouping Information Using the Tukey Method and 95% Confidence

Filler Content (wt%)_2	N	Mean	Grouping
0.4	5	68.7062	A
0.3	5	64.4446	B
0.2	5	59.682	C
0.05	5	43.6922	D
0	5	40.9414	D

(b)

Analysis of Variance

Source	DF	Adj SS	Adj MS	F-Value	P-Value
Filler Content (wt%)_1	4	28.2182	7.05456	99.51	<0.0001
Error	20	1.4179	0.07089		
Total	24	29.6361			

Means

Filler Content (wt%)_1	N	Mean	StDev	95% CI
0	5	5.2902	0.3482	(5.0418, 5.5386)
0.05	5	5.8184	0.2290	(5.5700, 6.0668)
0.2	5	2.7864	0.2629	(2.5380, 3.0348)
0.3	5	5.31640	0.21475	(5.06801, 5.56479)
0.4	5	5.0400	0.2561	(4.7916, 5.2884)

Pooled StDev = 0.266260

Grouping Information Using the Tukey Method and 95% Confidence

Filler Content (wt%)_1	N	Mean	Grouping
0.05	5	5.8184	A
0.3	5	5.31640	A B
0	5	5.2902	B
0.4	5	5.0400	B
0.2	5	2.7864	C

Table 7 Tukey method statistical data for OTR

Analysis of Variance

Source	DF	Adj SS	Adj MS	F-Value	P-Value
film	4	780717	195179	62.85	<0.0001
Error	14	43474	3105		
Total	18	824191			

Means

film	N	Mean	StDev	95% CI
0	3	729.09	114.38	(660.09, 798.10)
0.05	4	739.96	54.50	(680.20, 799.72)
0.2	4	542.80	49.93	(483.04, 602.56)
0.3	4	324.406	8.523	(264.647, 384.165)
0.4	4	243.724	15.321	(183.965, 303.483)

Pooled StDev = 55.7249

Grouping Information Using the Tukey Method and 95% Confidence

film	N	Mean	Grouping		
0.05	4	739.96	A		
0	3	729.09	A		
0.2	4	542.80		B	
0.3	4	324.406			C
0.4	4	243.724			C

Figures

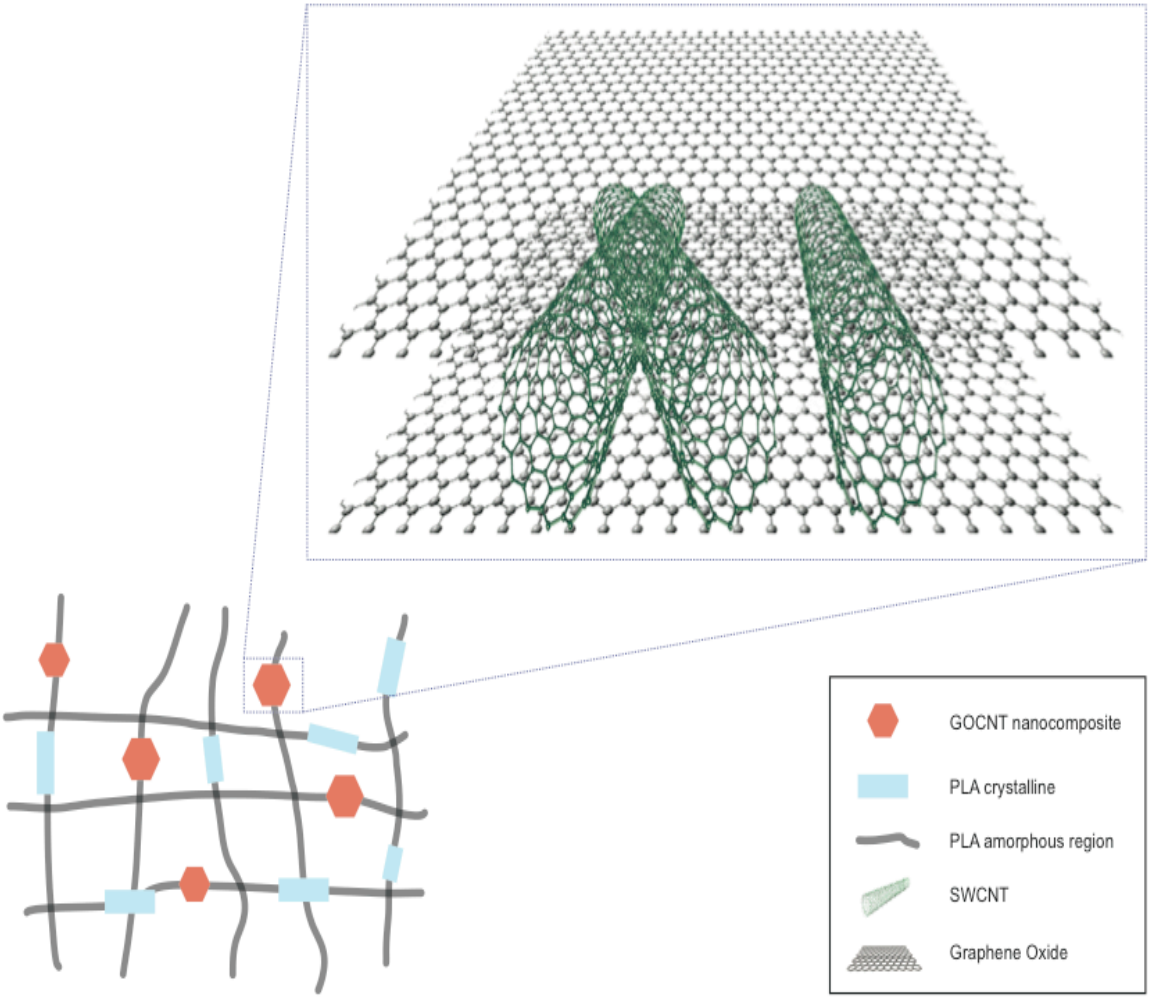

Figure 1. Representation of interaction of the GOCNT nanocomposite with poly(lactic acid)

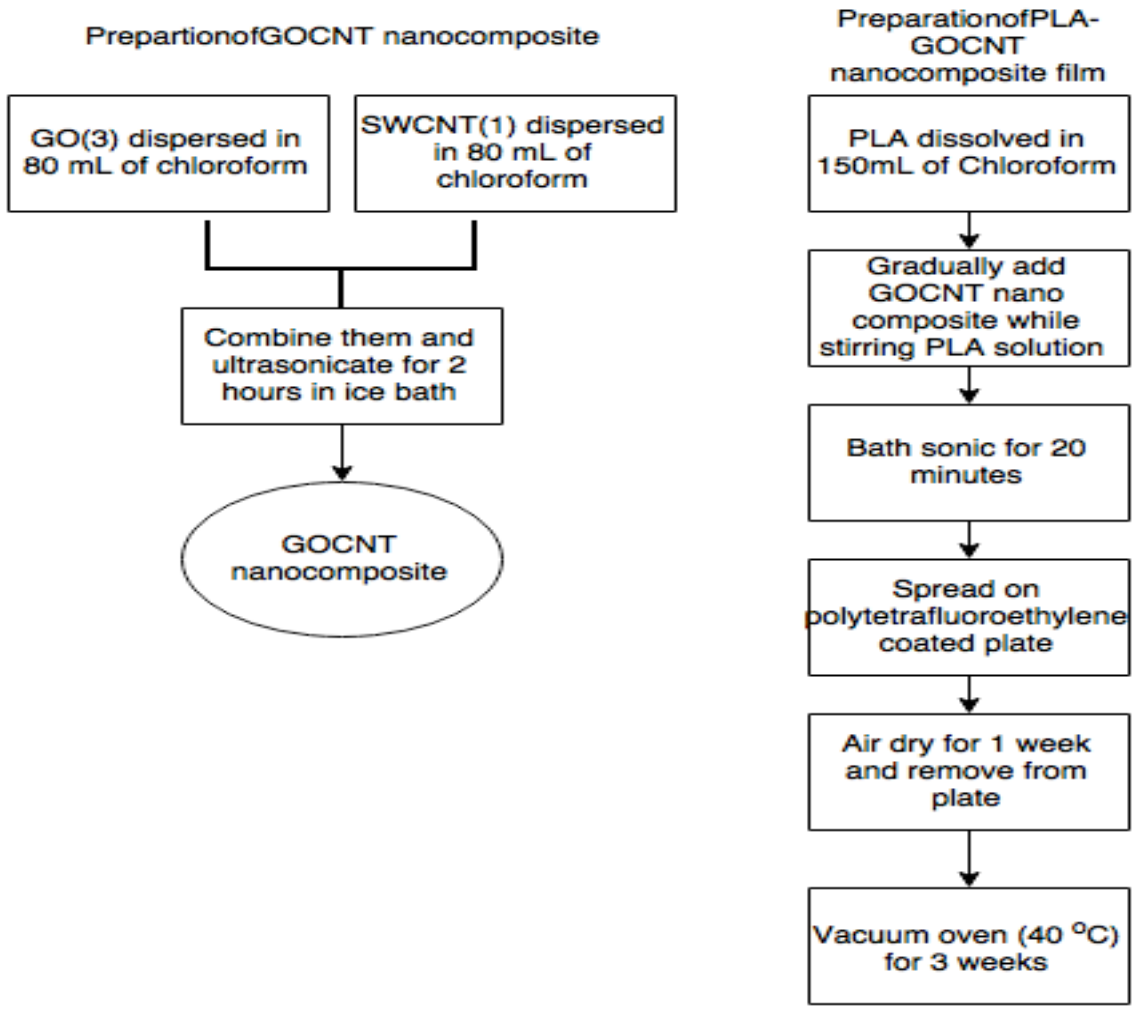

Figure 2. Preparation of PLA-GOCNT nanocomposite film

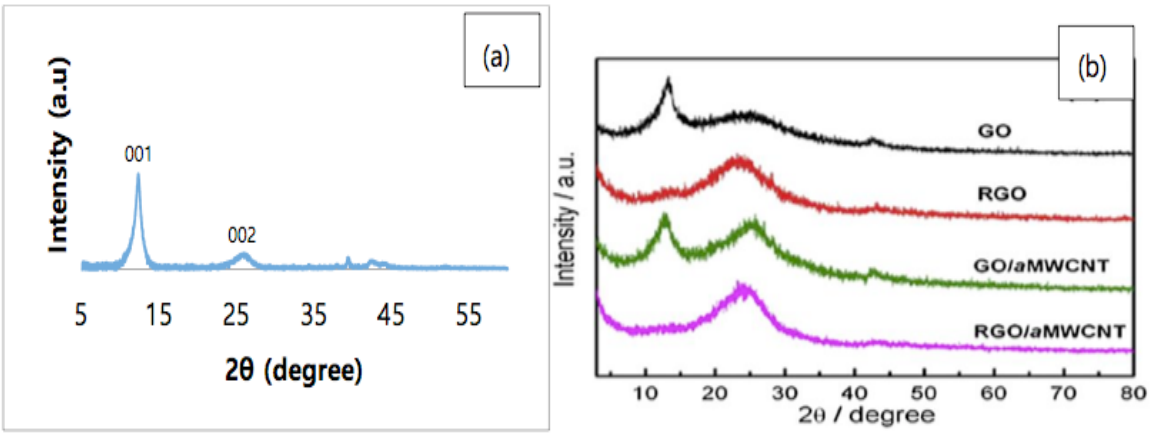

Figure 3. (a) XRD patterns of GOCNT composite (b) XRD patterns of GO/aMWCNT from researcher Sun and Wang

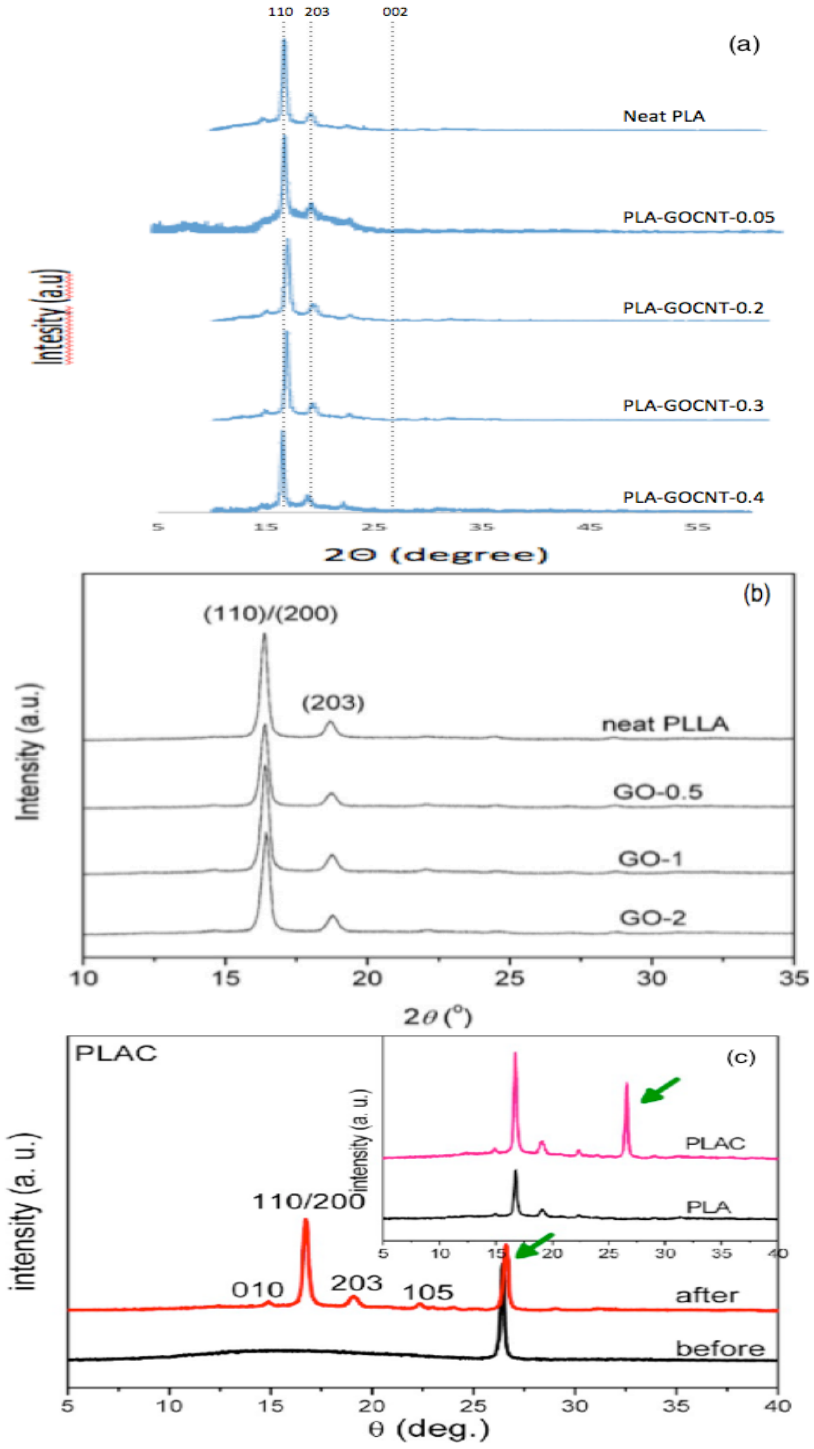

Figure 4. (a) XRD patterns of neat PLA film and PLA-GOCNT nanocomposite films (b) XRD patterns of neat PLA film and PLA-GO nanocomposite by Wang et al. (c) XRD patterns of PLA-GO nanocomposite by Wu et al.

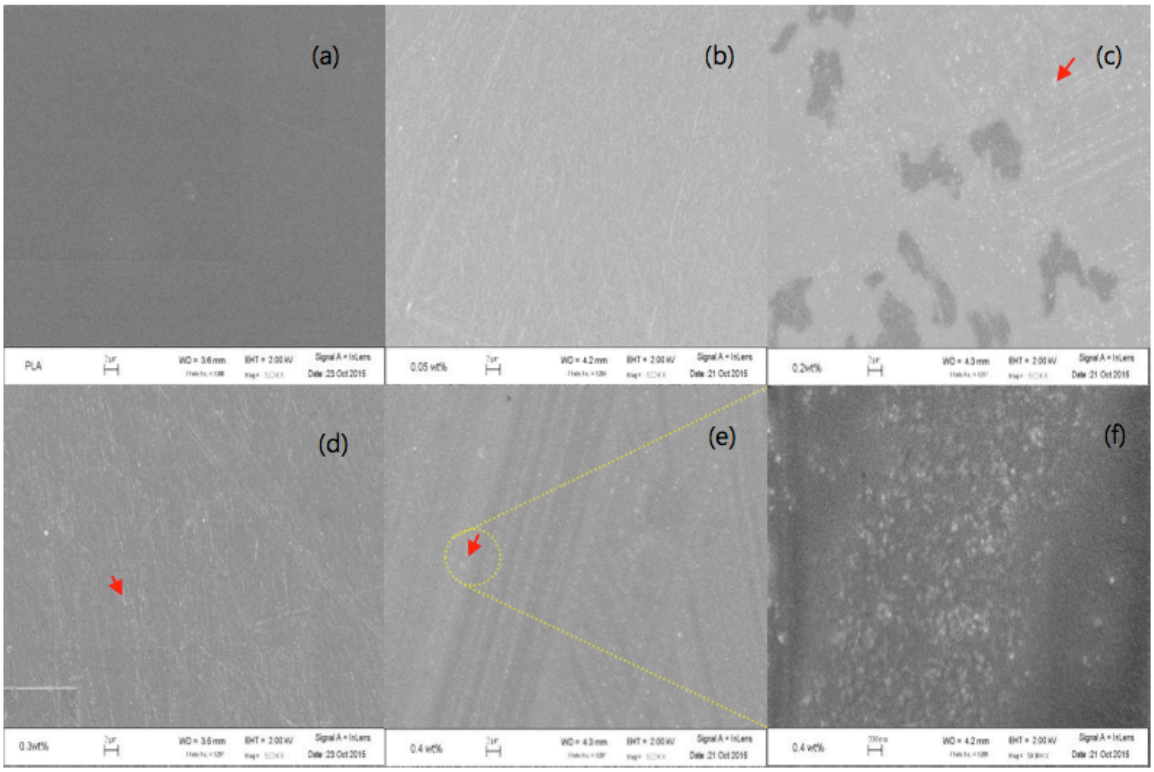

Figure 5. FESEM image of (a) neat PLA, (b) PLA-GOCNT-0.05, (c) PLA-GOCNT-0.2, (d) PLA-GOCNT-0.3, (e) PLA-GOCNT-0.4 and (f) x50 magnified PLA-GOCNT-0.4

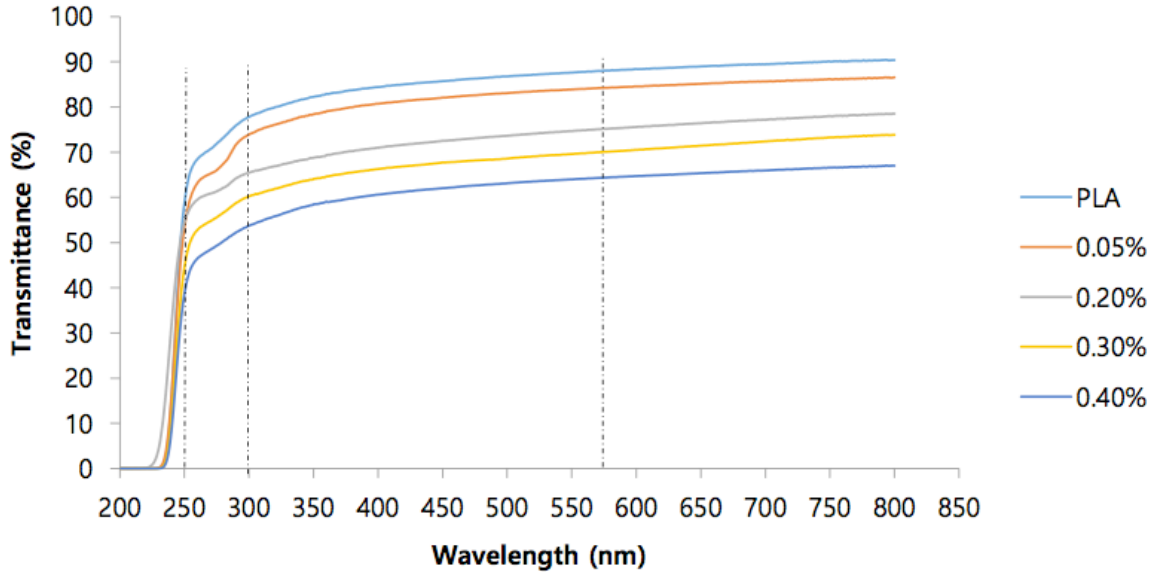

Figure 6. UV spectrophotometer graph

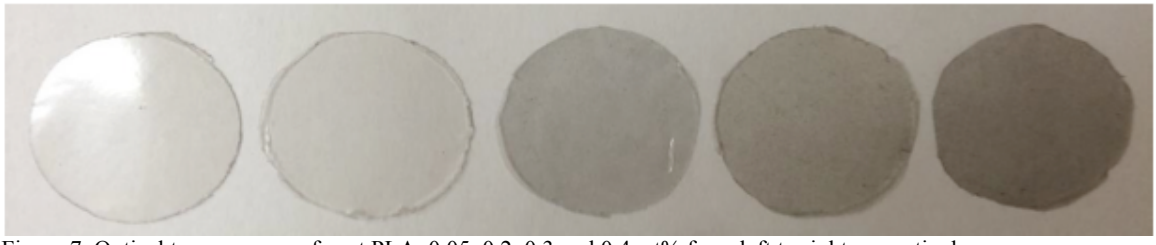

Figure 7. Optical transparency of neat PLA, 0.05, 0.2, 0.3 and 0.4 wt% from left to right respectively

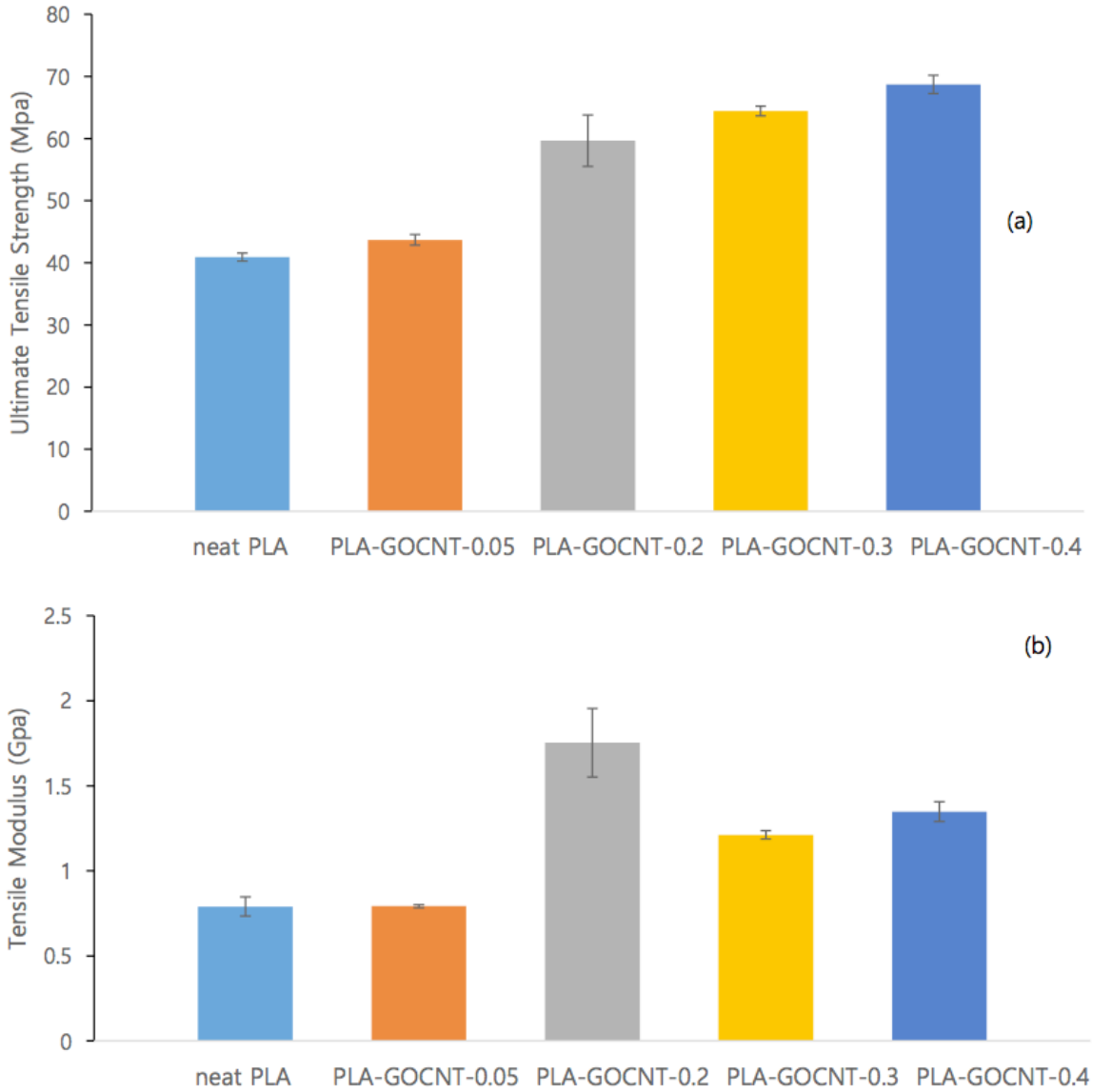

Figure 8. (a) Ultimate tensile strength and (b) tensile modulus for neat PLA and PLA-GOCNT nanocomposite films

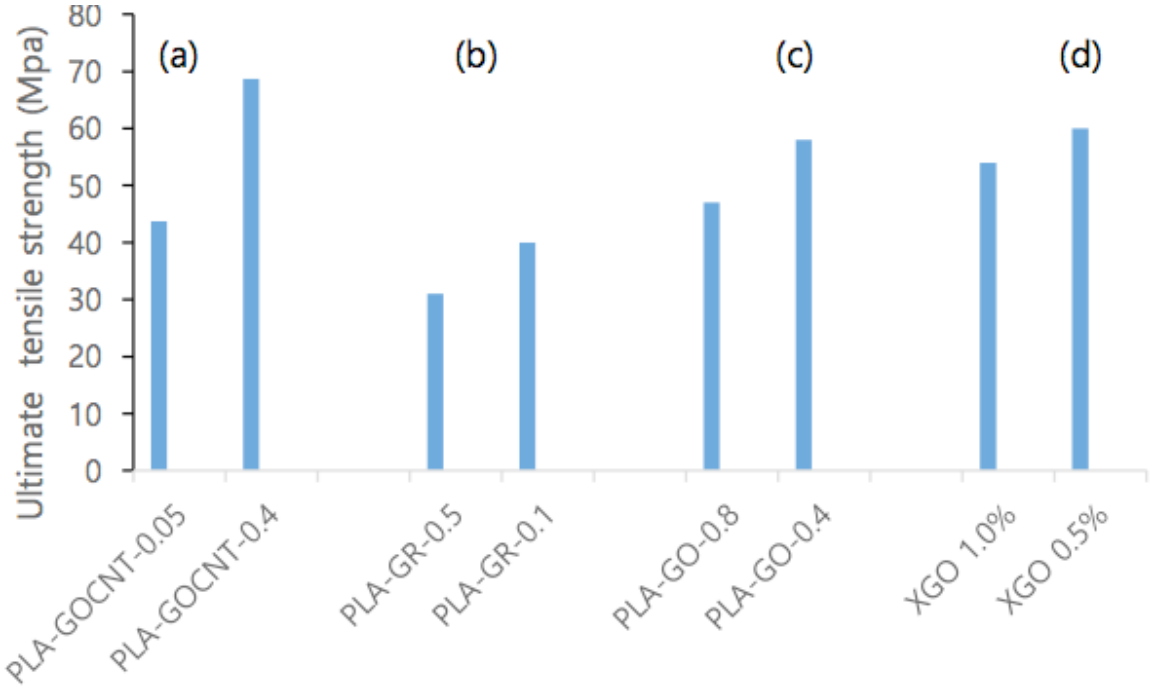

Figure 9. UTS comparison with others (a) PLA-GOCNT nanocomposite film (b) 0.5 and 0.1 wt% of GO by Valapa et al. (c) 0.2 and 0.4 wt% of GO by Pinto et al. (d) 1.0 and 0.5 wt% of GO by Buasri et al.

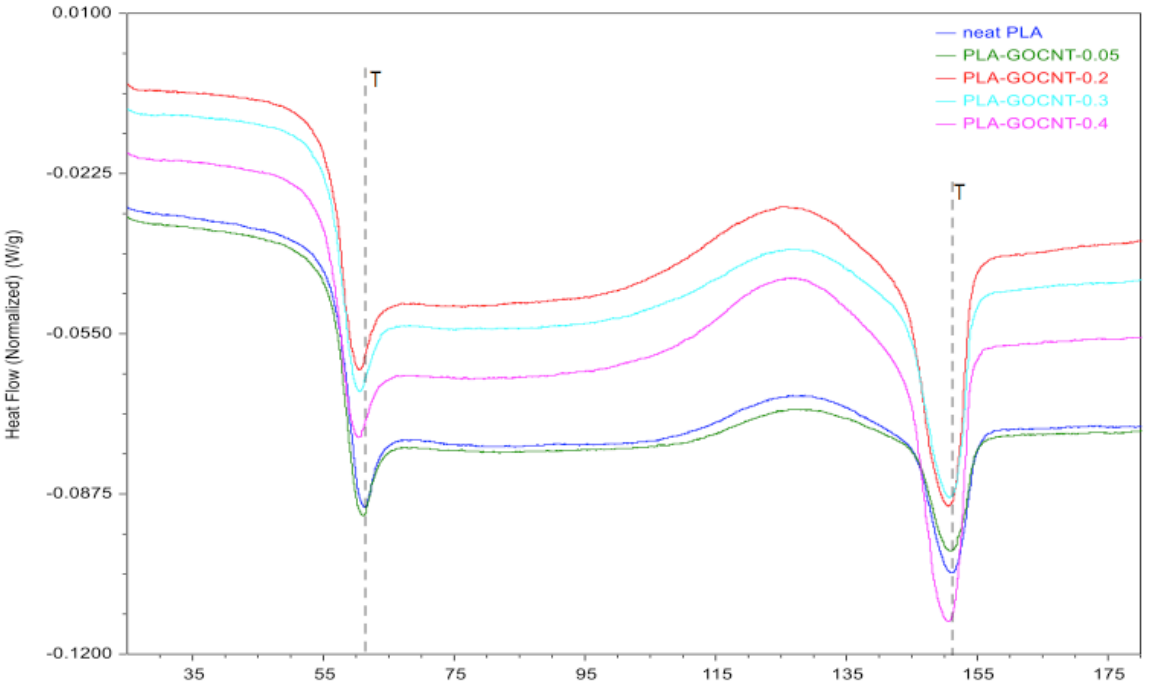

Figure 10. DSC second heating thermographs for neat PLA and PLA-GOCNT nanocomposite films at heating rate of 5 $^{o}C\ min^{-1}$

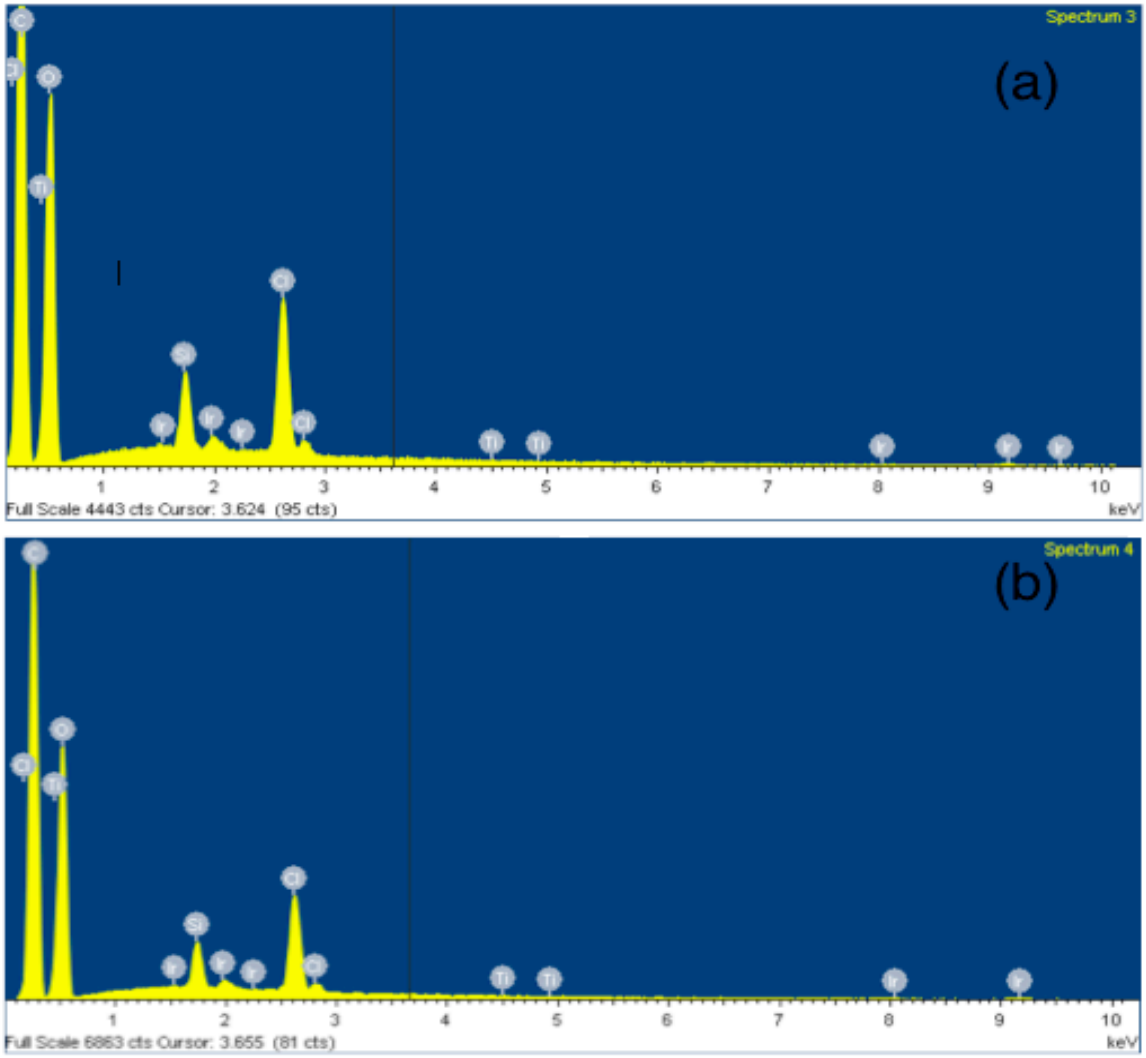

Figure 11. EDS maps of randomly selected regions of GOCNT nanocomposite (a) region 1 and (b) region 2.

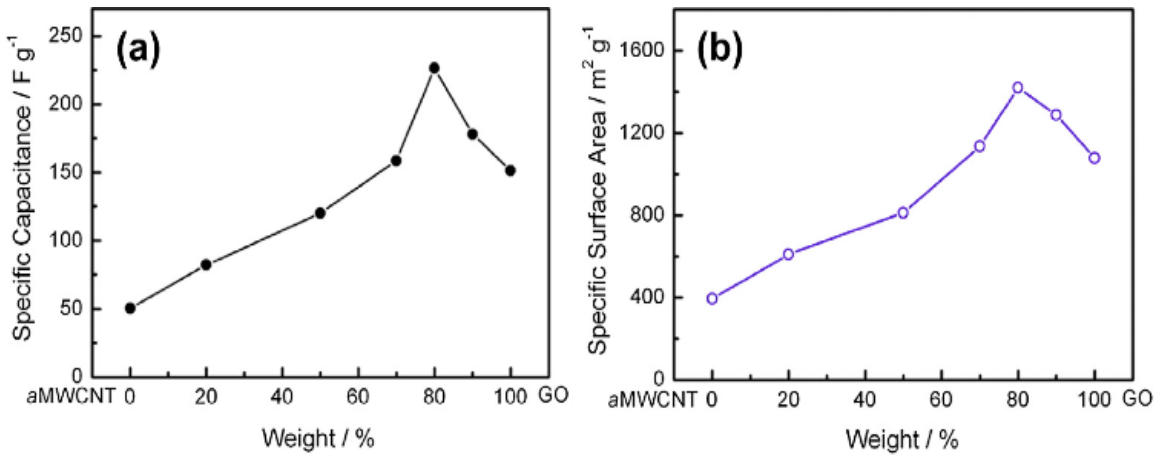

Figure 12. Influence of GO/aMWCNT weight ratio on (a) the specific capacitance and (b) the specific surface area of GO/aMWCNT (Sun, Wang et al. 2014).

References

Ajioka, M., et al. (1995). "BASIC PROPERTIES OF POLYLACTIC ACID PRODUCED BY THE DIRECT CONDENSATION POLYMERIZATION OF LACTIC-ACID." Bulletin of the Chemical Society of Japan 68(8): 2125-2131.

Alboofetileh, M., et al. (2013). "Effect of montmorillonite clay and biopolymer concentration on the physical and mechanical properties of alginate nanocomposite films." Journal of Food Engineering 117(1): 26-33.

Allen, M. J., et al. (2008). "Temperature dependent Raman spectroscopy of chemically derived graphene." Applied Physics Letters 93(19).

Allen, M. J., et al. (2010). "Honeycomb Carbon: A Review of Graphene." Chemical Reviews 110(1): 132-145.

B.K., A. (1991). X-ray Spectroscopy. Berlin, Springer-verlag.

Bao, L., et al. (2006). "Gas permeation properties of poly(lactic acid) revisited." Journal of Membrane Science 285(1-2): 166-172.

Barlow, C. Y. and D. C. Morgan (2013). "Polymer film packaging for food: An environmental assessment." Resources, Conservation and Recycling 78(0): 74-80.

Bourlinos, A. B., et al. (2003). "Graphite oxide: Chemical reduction to graphite and surface modification with primary aliphatic amines and amino acids." Langmuir 19(15): 6050-6055.

Braunecker, W. A. and K. Matyjaszewski (2007). "Controlled/living radical polymerization: Features, developments, and perspectives." Progress in Polymer Science 32(1): 93-146.

Buasri, A., et al. (2015). "The production and properties of polylactide (PLA) nanocomposites filled with graphene oxide (XGO)." Optoelectronics and Advanced Materials-Rapid Communications 9(3-4): 507-510.

Buchholz, B. (1994). 302, 694.

Cao, Y., et al. (2010). "Preparation of organically dispersible graphene nanosheet powders through a lyophilization method and their poly(lactic acid) composites." Carbon 48(13): 3834-3839.

Carrasco, F., et al. (2006). "Thermal stability of polyhydroxyalkanoates." Journal of Applied Polymer Science 100(3): 2111-2121.

Carrasco, F., et al. (2010). "Processing of poly(lactic acid): Characterization of chemical structure, thermal stability and mechanical properties." Polymer Degradation and Stability 95(2): 116-125.

Chen, D., et al. (2010). "In Situ Thermal Preparation of Polyimide Nanocomposite Films Containing

Functionalized Graphene Sheets." Acs Applied Materials & Interfaces 2(12): 3702-3708.

Chen, J.-T., et al. (2014). "Enhancing polymer/graphene oxide gas barrier film properties by introducing new crystals." Carbon 75: 443-451.

Chollet, E., et al. (2009). "Monitoring nisin desorption from a multi-layer polyethylene-based film coated with nisin loaded HPMC film and diffusion in agarose gel by an immunoassay (ELISA) method and a numerical modeling." Innovative Food Science & Emerging Technologies 10(2): 208-214.

Compton, O. C., et al. (2010). "Crumpled Graphene Nanosheets as Highly Effective Barrier Property Enhancers." Advanced Materials 22(42): 4759-+.

D. Sawai, K. T., A. Sasashige, T. Kanamoto and S.H. Hyon (2003). "Macromolecules." 36: 3601-3605.

Dash, T. K. and V. B. Konkimalla (2012). "Polymeric Modification and Its Implication in Drug Delivery: Poly-epsilon-caprolactone (PCL) as a Model Polymer." Molecular Pharmaceutics 9(9): 2365-2379.

Datta, R. and M. Henry (2006). "Lactic acid: recent advances in products, processes and technologies — a review." Journal of Chemical Technology & Biotechnology 81(7): 1119-1129.

Doi, Y., et al. (1990). "BIODEGRADATION OF MICROBIAL COPOLYESTERS - POLY(3-HYDROXYBUTYRATE-CO-3-HYDROXYVALERATE) AND POLY(3-HYDROXYBUTYRATE-CO-4-HYDROXYBUTYRATE)." Macromolecules 23(1): 26-31.

Dorgan, J. R., et al. (2000). "Thermal and rheological properties of commercial-grade poly(lactic acid)s." Journal of Polymers and the Environment 8(1): 1-9.

Dresselhaus, M. S. and G. Dresselhaus (2002). "Intercalation compounds of graphite." Advances in Physics 51(1): 1-186.

Dreyer, D. R., et al. (2010). "The chemistry of graphene oxide." Chemical Society Reviews 39(1): 228-240.

Du, J. and H.-M. Cheng (2012). "The Fabrication, Properties, and Uses of Graphene/Polymer Composites." Macromolecular Chemistry and Physics 213(10-11): 1060-1077.

Fang, M., et al. (2009). "Covalent polymer functionalization of graphene nanosheets and mechanical properties of composites." Journal of Materials Chemistry 19(38): 7098-7105.

Fernandez-Merino, M. J., et al. (2010). "Vitamin C Is an Ideal Substitute for Hydrazine in the Reduction of Graphene Oxide Suspensions." Journal of Physical Chemistry C 114(14): 6426-6432.

Fu, Y., et al. (2014). "Functionalized graphenes with polymer toughener as novel interface modifier for property-tailored polylactic acid/graphene nanocomposites." Polymer 55(24): 6381-6389.

G. B. Kharas, F. S.-R., and D. K. Severson (1994). Plastics From Microbes: pp. 93-137.

Gao, J., et al. (2010). "Environment-Friendly Method To Produce Graphene That Employs Vitamin C and Amino Acid." Chemistry of Materials 22(7): 2213-2218.

Garlotta, D. (2001). "A literature review of poly(lactic acid)." Journal of Polymers and the Environment 9(2): 63-84.

Geim, A. K. and K. S. Novoselov (2007). "The rise of graphene." Nature Materials 6(3): 183-191.

Giles FH, W. J., Mount EM (2005). Extrusion, the definitive processing guide and handbook.

Gironi, F. and V. Piemonte (2011). "Bioplastics and Petroleum-based Plastics: Strengths and Weaknesses." Energy Sources Part a-Recovery Utilization and Environmental Effects 33(21): 1949-1959.

Goenka, S., et al. (2014). "Graphene-based nanomaterials for drug delivery and tissue engineering." Journal of Controlled Release 173: 75-88.

Guo, H., et al. (2013). "Preparation of reduced graphene oxide by infrared irradiation induced photothermal reduction." Nanoscale 5(19): 9040-9048.

Gupta, A., et al. (2006). "Raman scattering from high-frequency phonons in supported n-graphene layer films." Nano Letters 6(12): 2667-2673.

Hartmann, M. H. (1998). Biopolymers from Renewable Resources Springer-Verlag, Berlin.

Hassan, M., et al. (2013). "High-yield aqueous phase exfoliation of graphene for facile nanocomposite synthesis via emulsion polymerization." Journal of Colloid and Interface Science 410: 43-51.

Hassouna, F., et al. (2011). "Development of new approach based on Raman spectroscopy to study the dispersion of expanded graphite in poly(lactide)." Polymer Degradation and Stability 96(12): 2040-2047.

Hofmann, U. and R. Holst (1939). "The acidic nature and the methylation of graphitoxide." Berichte Der Deutschen Chemischen Gesellschaft 72: 754-771.

Hu, K., et al. (2014). "Graphene-polymer nanocomposites for structural and functional applications." Progress in Polymer Science 39(11): 1934-1972.

Huang, H.-D., et al. (2014). "Improved barrier properties of poly(lactic acid) with randomly dispersed graphene oxide nanosheets." Journal of Membrane Science 464: 110-118.

Hummers, W. S. and R. E. Offeman (1958). "PREPARATION OF GRAPHITIC OXIDE." Journal of the American Chemical Society 80(6): 1339-1339.

Iannace, S. and L. Nicolais (1997). "Isothermal crystallization and chain mobility of poly(L-lactide)." Journal of Applied Polymer Science 64(5): 911-919.

Inata, H. and S. Matsumura (1985). "CHAIN EXTENDERS FOR POLYESTERS .1. ADDITION-TYPE CHAIN EXTENDERS REACTIVE WITH CARBOXYL END GROUPS OF POLYESTERS." Journal of Applied Polymer Science 30(8): 3325-3337.

J. K. Lalla, N. N. C. (1990). Indian Drugs 27(10), 516-522.

Jamshidian, M., et al. (2010). "Poly-Lactic Acid: Production, Applications, Nanocomposites, and Release Studies." Comprehensive Reviews in Food Science and Food Safety 9(5): 552-571.

Jin, J., et al. (2013). "Identifying the Active Site in Nitrogen-Doped Graphene for the VO2+/VO2+ Redox Reaction." ACS Nano 7(6): 4764-4773.

Jin, T., et al. (2009). "Antimicrobial activity of nisin incorporated in pectin and polylactic acid composite films against Listeria monocytogenes." International Journal of Food Science and Technology 44(2): 322-329.

Kawai, T., et al. (2007). "Crystallization and melting behavior of poly (L-lactic acid)." Macromolecules 40(26): 9463-9469.

Kim, I.-H. and Y. G. Jeong (2010). "Polylactide/Exfoliated Graphite Nanocomposites with Enhanced Thermal Stability, Mechanical Modulus, and Electrical Conductivity." Journal of Polymer Science Part B-Polymer Physics 48(8): 850-858.

Kim, Y., et al. (2009). "Transparent nanocomposites prepared by incorporating microbial nanofibrils into poly(L-lactic acid)." Current Applied Physics 9: S69-S71.

Kopinke, F. D., et al. (1996). "Thermal decomposition of biodegradable polyesters .2. Poly(lactic acid)." Polymer Degradation and Stability 53(3): 329-342.

Kricheldorf, H. R. and A. Serra (1985). "POLYLACTONES .6. INFLUENCE OF VARIOUS METAL-SALTS ON THE OPTICAL PURITY OF POLY(L-LACTIDE)." Polymer Bulletin 14(6): 497-502.

Krikorian, V. and D. J. Pochan (2004). "Unusual crystallization behavior of organoclay reinforced poly(L-lactic acid) nanocomposites." Macromolecules 37(17): 6480-6491.

L. Liu, T. Z. J., D. R. Coffin and K. B. Hicks (2009). "J. Agric. Food Chem." 57(8392-8398).

Land, T. A., et al. (1992). "STM INVESTIGATION OF SINGLE LAYER GRAPHITE STRUCTURES PRODUCED ON PT(111) BY HYDROCARBON DECOMPOSITION." Surface Science 264(3): 261-270.

Lape, N. K., et al. (2004). "Polydisperse flakes in barrier films." Journal of Membrane Science 236(1–2): 29-37.

Lee, S.-Y. and S.-J. Park (2014). "Isothermal exfoliation of graphene oxide by a new carbon dioxide pressure swing method." Carbon 68(0): 112-117.

Lehermeier, H. J., et al. (2001). "Gas permeation properties of poly(lactic acid)." Journal of Membrane Science 190(2): 243-251.

Lei, L., et al. (2012). "Preparing conductive poly(lactic acid) (PLA) with poly(methyl methacrylate) (PMMA) functionalized graphene (PFG) by admicellar polymerization." Chemical Engineering Journal 209: 20-27.

Lerf, A., et al. (1998). "Structure of graphite oxide revisited." Journal of Physical Chemistry B 102(23): 4477-4482.

Li, J. L., et al. (2006). "Oxygen-driven unzipping of graphitic materials." Physical Review Letters 96(17).

Li, Y., et al. (2009). "Crystallization Improvement of Poly(L-lactide) Induced by Functionalized Multiwalled Carbon Nanotubes." Journal of Polymer Science Part B-Polymer Physics 47(3): 326-339.

Loh, K. P., et al. (2010). "Graphene oxide as a chemically tunable platform for optical applications." Nature Chemistry 2(12): 1015-1024.

Lopez-Rubio, A., et al. (2004). "Overview of active polymer-based packaging technologies for food applications." Food Reviews International 20(4): 357-387.

Lunt, J. (1998). "Large-scale production, properties and commercial applications of polylactic acid polymers." Polymer Degradation and Stability 59(1-3): 145-152.

Lv, R. T., et al. (2014). "Building Complex Hybrid Carbon Architectures by Covalent Interconnections: Graphene-Nanotube Hybrids and More." ACS Nano 8(5): 4061-4069.

M. Murariu, A. L. D., L. Bonnaud, Y. Paint, A. Gallos, G. Fontaine, S. Bourbigot and P. Dubois, (2010). "Polym. Degrad. Stab." 95: 889-900.

Mehta R, K. V., Bhunia H, Upadhyay SN (2005). "Synthesis of poly(lactic acid): a reveiw." J Macromol Sci Polym Rev 45:325-49.

Mermin, N. D. (1968). "CRYSTALLINE ORDER IN 2 DIMENSIONS." Physical Review 176(1): 250-&.

Mohanty, A. K., et al. (2002). "Sustainable Bio-Composites from Renewable Resources: Opportunities and Challenges in the Green Materials World." Journal of Polymers and the Environment 10(1-2): 19-26.

Mohanty, A. K., et al. (2000). "Biofibres, biodegradable polymers and biocomposites: An overview." Macromolecular Materials and Engineering 276-277(1): 1-24.

Murariu, M., et al. (2010). "The production and properties of polylactide composites filled with expanded graphite." Polymer Degradation and Stability 95(5): 889-900.

Nakayama, N. and T. Hayashi (2007). "Preparation and characterization of poly(L-lactic acid)/TiO2 nanoparticle nanocomposite films with high transparency and efficient photodegradability." Polymer Degradation and Stability 92(7): 1255-1264.

Norazlina, H. and Y. Kamal (2015). "Graphene modifications in polylactic acid nanocomposites: a review." Polymer Bulletin 72(4): 931-961.

Novoselov, K. S., et al. (2012). "A roadmap for graphene." Nature 490(7419): 192-200.

Novoselov, K. S., et al. (2005). "Two-dimensional gas of massless Dirac fermions in graphene." Nature 438(7065): 197-200.

Novoselov, K. S., et al. (2005). "Two-dimensional atomic crystals." Proceedings of the National Academy of Sciences of the United States of America 102(30): 10451-10453.

Partoens, B. and F. M. Peeters (2006). "From graphene to graphite: Electronic structure around the K point." Physical Review B 74(7).

Patel, M. (2002). "Life cycle assessment of synthetic and biological polyesters." Proceedings of the International Symposium on Biological Polyesters, Munster, Germany,.

Pei, S. and H.-M. Cheng (2012). "The reduction of graphene oxide." Carbon 50(9): 3210-3228.

Peierls, R. E. (1935). "Quelques proprietes typiques des corpses solides." Ann. I. H. Poincare 5, 177-222.

Pinto, A. M., et al. (2013). "Effect of incorporation of graphene oxide and graphene nanoplatelets on mechanical and gas permeability properties of poly(lactic acid) films." Polymer International 62(1): 33-40.

Pocas, M. F., et al. (2008). "A Critical Survey of Predictive Mathematical Models for Migration from Packaging." Critical Reviews in Food Science and Nutrition 48(10): 913-928.

Pu, N.-W., et al. (2009). "Production of few-layer graphene by supercritical CO2 exfoliation of graphite." Materials Letters 63(23): 1987-1989.

Qiu, J., et al. (2008). "New insights into the multiple melting behaviors of the semicrystalline ethylene-hexene copolymer: Origins of quintuple melting peaks." Journal of Polymer Science Part B-Polymer Physics 46(19): 2100-2115.

R. Valapa, G. P. a. V. K. (2014). "Int. J. Biol. Macromol." 65: 275-284.

Raquez, J.-M., et al. (2013). "Polylactide (PLA)-based nanocomposites." Progress in Polymer Science 38(10–11): 1504-1542.

Reed, S. J. B. (1993). Electron Microprobe Analysis. C. U. Press. Cambridge.

Roy, N., et al. (2012). "Modifications of carbon for polymer composites and nanocomposites." Progress in Polymer Science 37(6): 781-819.

Ruess, G. (1946). "Uber das Graphitoxyhydroxyd (Graphitoxyd)." Monatshefte Chem 76: 381-417.

Russ, J. C. (1984). Fundamentals of Energy Dispersive X-ray Analysis. London, Butterworths.

Scholz, W. and H. P. Boehm (1969). "GRAPHITE OXIDE .6. STRUCTURE OF GRAPHITE OXIDE." Zeitschrift Fur Anorganische Und Allgemeine Chemie 369(3-6): 327-&.

Schrand, A. (2005). "Polymer Sample Preparation for Electron Microscopy." Microscopy and Microanalysis 11(SupplementS02): 702-703.

Scott, A. (2000). Chem. Week.

Segal, M. (2009). "Selling graphene by the ton." Nature Nanotechnology 4(10): 611-613.

Shen, H., et al. (2012). "Biomedical Applications of Graphene." Theranostics 2(3): 283-294.

Shogren, R. (1997). "Water vapor permeability of biodegradable polymers." Journal of Environmental Polymer Degradation 5(2): 91-95.

Singha, A. S. and V. K. Thakur (2012). BIOPOLYMERS FROM RENEWABLE RESOURCES: AN INTRODUCTION.

Siracusa, V., et al. (2008). "Biodegradable polymers for food packaging: a review." Trends in Food Science & Technology 19(12): 634-643.

Spinu, M., et al. (1996). "Material design in poly(lactic acid) systems: Block copolymers, star homo- and copolymers, and stereocomplexes." Journal of Macromolecular Science-Pure and Applied Chemistry A33(10): 1497-1530.

Suk, J. W., et al. (2010). "Mechanical Properties of Mono layer Graphene Oxide." ACS Nano 4(11): 6557-6564.

Sun, M., et al. (2014). "Irradiation preparation of reduced graphene oxide/carbon nanotube composites for high-performance supercapacitors." Journal of Power Sources 245: 436-444.

Szabo, T., et al. (2006). "Evolution of surface functional groups in a series of progressively oxidized graphite oxides." Chemistry of Materials 18(11): 2740-2749.

Terrones, M., et al. (2010). "Graphene and graphite nanoribbons: Morphology, properties, synthesis, defects and applications." Nano Today 5(4): 351-372.

Tian, L., et al. (2010). "Graphene Oxides for Homogeneous Dispersion of Carbon Nanotubes." Acs Applied

Materials & Interfaces 2(11): 3217-3222.

Tsuji, H., et al. (2006). "Water vapor permeability of poly(lactide)s: Effects of molecular characteristics and crystallinity." Journal of Applied Polymer Science 99(5): 2245-2252.

Valapa, R. B., et al. (2015). "Effect of graphene content on the properties of poly(lactic acid) nanocomposites." Rsc Advances 5(36): 28410-28423.

Valapa, R. B., et al. (2015). "Fabrication and Characterization of Sucrose Palmitate Reinforced Poly(lactic acid) Bionanocomposite Films." Journal of Applied Polymer Science 132(3).

Vanderweij, F. W. (1980). "THE ACTION OF TIN-COMPOUNDS IN CONDENSATION-TYPE RTV SILICONE RUBBERS." Makromolekulare Chemie-Macromolecular Chemistry and Physics 181(12): 2541-2548.

Wachsen, O., et al. (1997). "Thermal degradation of poly-L-lactide - Studies on kinetics, modelling and melt stabilisation." Polymer Degradation and Stability 57(1): 87-94.

Wang, H. and Z. Qiu (2011). "Crystallization behaviors of biodegradable poly(L-lactic acid)/graphene oxide nanocomposites from the amorphous state." Thermochimica Acta 526(1-2): 229-236.

Wang, R., et al. (2011). "Fibrous nanocomposites of carbon nanotubes and graphene-oxide with synergetic mechanical and actuative performance." Chemical Communications 47(30): 8650-8652.

Williams, G. and P. V. Kamat (2009). "Graphene-Semiconductor Nanocomposites: Excited-State Interactions between ZnO Nanoparticles and Graphene Oxide." Langmuir 25(24): 13869-13873.

Wu, D., et al. (2013). "Crystallization Behavior of Polylactide/Graphene Composites." Industrial & Engineering Chemistry Research 52(20): 6731-6739.

Xu, J.-Z., et al. (2010). "Isothermal Crystallization of Poly(L-lactide) Induced by Graphene Nanosheets and Carbon Nanotubes: A Comparative Study." Macromolecules 43(11): 5000-5008.

Yang, J.-H., et al. (2012). "Preparation and characterization of poly(L-lactide)-graphene composites using the in situ ring-opening polymerization of PLLA with graphene as the initiator." Journal of Materials Chemistry 22(21): 10805-10815.

Yates, M. R. and C. Y. Barlow (2013). "Life cycle assessments of biodegradable, commercial biopolymers-A critical review." Resources Conservation and Recycling 78: 54-66.

Yoon, O. J., et al. (2011). "Nanocomposite nanofibers of poly(D, L-lactic-co-glycolic acid) and graphene oxide nanosheets." Composites Part a-Applied Science and Manufacturing 42(12): 1978-1984.

Yoshimura, N. (2014). Introduction of the Electron Microscope. Historical Evolution toward Achieving Ultrahigh Vacuum in Jeol Electron Microscopes: 1-10.